Application of Multi-Seismic Attributes in Estimating Reservoir Properties

by

Maher Ibraheem Al-Marhoun

A Thesis Presented to the

FACULTY OF THE COLLEGE OF GRADUATE STUDIES

KING FAHD UNIVERSITY OF PETROLEUM & MINERALS

DHAHRAN, SAUDI ARABIA

In Partial Fulfillment of the
Requirements for the Degree of

MASTER OF SCIENCE

In

GEOLOGY

September, 1997

INFORMATION TO USERS

This manuscript has been reproduced from the microfilm master. UMI films the text directly from the original or copy submitted. Thus, some thesis and dissertation copies are in typewriter face, while others may be from any type of computer printer.

The quality of this reproduction is dependent upon the quality of the copy submitted. Broken or indistinct print, colored or poor quality illustrations and photographs, print bleedthrough, substandard margins, and improper alignment can adversely affect reproduction.

In the unlikely event that the author did not send UMI a complete manuscript and there are missing pages, these will be noted. Also, if unauthorized copyright material had to be removed, a note will indicate the deletion.

Oversize materials (e.g., maps, drawings, charts) are reproduced by sectioning the original, beginning at the upper left-hand corner and continuing from left to right in equal sections with small overlaps. Each original is also photographed in one exposure and is included in reduced form at the back of the book.

Photographs included in the original manuscript have been reproduced xerographically in this copy. Higher quality 6" x 9" black and white photographic prints are available for any photographs or illustrations appearing in this copy for an additional charge. Contact UMI directly to order.

UMI

A Bell & Howell Information Company
300 North Zeeb Road, Ann Arbor MI 48106-1346 USA
313/761-4700 800/521-0600

Application of Multi-Seismic Attributes in Estimating Reservoir Properties

BY

Maher Ibraheem Al-Marhoun

A Thesis Presented to the

FACULTY OF THE COLLEGE OF GRADUATE STUDIES

KING FAHD UNIVERSITY OF PETROLEUM & MINERALS

DHAHRAN, SAUDI ARABIA

In Partial Fulfillment of the
Requirements for the Degree of

MASTER OF SCIENCE

In

GEOLOGY

September, 1997

KING FAHD UNIVERSITY OF PETROLEUM AND MINERALS
DHAHRAN 31261, SAUDI ARABIA

COLLEGE OF GRADUATE STUDIES

This thesis, written by Maher Ibraheem Al-Marhoum under the direction of his Thesis Advisor and approved by his Thesis Committee, has been presented to and accepted by the Dean of the College of Graduate Studies, in partial fulfillment of the requirements for the degree of MASTER OF SCIENCE in GEOLOGY.

Thesis Committee

Dr. G. Korvin, Thesis Advisor

Dr. Z. Al-Harari, Member

Dr. A. Qahwash, Member

Department Chairman

Dean, College of Graduate Studies

Date

ACKNOWLEDGMENTS

I would like to thank the Ministry of Petroleum and Mineral Resources and Saudi ARAMCO for permission to publish this thesis. Mr. Mahmoud Abdul-Baqi, Vice President of Exploration Organization, Mr. Hani Abu Khadra, Manager of Geophysical Exploration, Dr. Kamal Al-Yahya, Manager of Exploration Application Services Department, Mr. Saleh Al-Maghlouth, Chief Geophysicist of Geophysical Technology Division, and Mr. John Emploliti, Chief Geophysicist of Processing Division are all acknowledged for providing data and support.

Thanks are due to Dr. Gabor Korvin, Committee Chairman, Dr. Abdellatif Qahwash, and Dr. Zaki Harari for guidance and support. Special thanks and appreciations are due to Dr. Mohammed Al-Fares who was of great help. Also thanks are due to Mr. Jamil Al-Hajhug for his help.

Finally, I would like to acknowledge all of the help, support, and encouragement provided by my family.

This thesis is dedicated to my father and mother.

TABLE OF CONTENTS

LIST OF TABLES

LIST OF FIGURES

المستخلص

الاسم : ماهر إبراهيم منصور المرهون

العنوان : استخدام عدة خصائص سيزموغرافية لتقدير الخصائص المكمنية

التخصص : جيولوجيا

التاريخ : سبتمبر 1997م

يمكن استخدام الخصائص السيزموغرافية في عملية تفسير البيانات السيزموغرافية. فكلما تطورت البيانات السيزموغرافية في دقتها كلما كان تفسير هذه البيانات وخصائصها اكثر صحة. إن الخصائص السيزموغرافية تظهر معلومات لا يمكن في معظم الأحيان اكتشافها من العروض السيزموغرافية الاعتيادية. كما يمكن استخدام هذه الخصائص في عملية التفسير الكمي و الكيفي للبيانات.

إن الهدف الرئيسي من هذه الدراسة هو تقدير المسامية، التشبع المائي و كمية الطمي باستخدام عدة خصائص سيزموغرافية ومن ثم الوصول إلى نتيجة واحدة اعتمادا على الدراستين الكمية والكيفية للبيانات.

في الدراسة الكمية، استخدمت تسع خصائص سيزموغرافية لتقدير خصائص المكمن المذكورة آنفا. حسبت متوسطات هذه الخصائص للطبقة من نهاية الكاربونات من متكون الخف إلى سطح اللاتوافق تحت متكون العنيزة، ثم قورنت بخصائص المكمن المحسوبة من بيانات تسع عشرة بئرا. قربت العلاقة بين الخصائص السيزموغرافية وخصائص المكمن بمعادلة خطية، ومن ثم طبقت هذه المعادلة على جميع البيانات.

في الدراسة الكيفية، درست الخصائص الطيفية للبيانات السيزموغرافية بالإضافة إلى الخصائص التسع المستخدمة في الدراسة الكمية. ثم استخدمت جميع هذه الخصائص لمعرفة جودة المكمن من الناحية الكيفية.

استخدمت البيانات من بئرين إضافيتين لم تستخدما في عملية تقدير الخصائص المكمنية لاختبار مشروعية الطريقة المستخدمة. وقد تبين انه باستطاعة الطريقة المستخدمة في هذا البحث تقدير قيم الخصائص المكمنية عند بئرا الاختبار. و بعد ذلك قورنت طريقة استخدام عدة خصائص سيزموغرافية من جهة بطريقة استخدام خاصية سيزموغرافية واحدة و بطريقة استخدام البيانات المجموعة من الآبار فقط من جهة أخرى.

درجة الماجستير في العلوم

جامعة الملك فهد للبترول والمعادن

الظهران – المملكة العربية السعودية

سبتمبر 1997م

ABSTRACT

Name:	Maher Ibraheem Al-Marhoun
Title:	Application of Multi-Seismic Attributes in Estimating Reservoir Properties
Major Field:	Geology
Date	September, 1997

Seismic attributes can be used in seismic interpretation. As seismic data quality improves, interpretation of seismic attributes becomes more reliable. Seismic attributes reveal information that often cannot be detected in conventional seismic displays. The attributes can be used for both quantitative and qualitative interpretation of any zone of interest.

The main goal of this study is to estimate porosity, water saturation, and volume of silt using several seismic attributes and then arrive at getting one conclusion based on the quantitative and the qualitative analyses.

In the quantitative analysis, nine seismic attributes are used to estimate the reservoir properties mentioned above. These attributes are calculated and averaged over the zone of interest, from Base Khuff to Pre Unayzah Unconformity, compared to the log derived reservoir properties from 19 wells. Multi-variant regression is used to approximate a linear transformation between seismic attributes and reservoir properties. Then the transformation is applied to the whole seismic data.

In the qualitative analysis, spectral attributes are studied in addition to the nine seismic attributes discussed in the quantitative analysis. Attributes are related to the reservoir properties qualitatively. Both the quantitative and the qualitative interpretation are in agreement.

I preserved two wells for validation purposes. The estimated reservoir properties of these two wells using Multi-seismic-attributes approach are in agreement with the well driven reservoir properties.The multi-seismic-attributes driven reservoir properties method was compared to the single-attribute method and to a method utilizing simple kriging of well information.

Master of Science Degree
King Fahd University of Petroleum and Minerals
Dhahran, Saudi Arabia
September 1997

CHAPTER 1 *Introduction*

In the past seismic data were conventionally used only to help in the structural interpretation of a specific area. Currently, there is a trend toward getting as much information as possible out of seismics, especially as its quality is getting better. Therefore, issues were raised about the possibility of extracting stratigraphic information and reservoir properties from seismic data.

Seismic data have much greater spatial resolution than that of well data. Therefore, if we could use it to guide the computation of reservoir properties between wells, the output would be more reliable than using geostatistical results of only well data to get these values because geostatistical methods depend on a probability model for the spatial variability of the reservoir properties.

Different types of algorithms such as inversion and attribute calculation algorithms were invented and used to get information about reservoir properties. All of these algorithms or methods intend to integrate available data such as geological, petrophysical, and geophysical data in order to determine the lithology or the reservoir properties.

In this research, several seismic attributes will be calculated on a specific interval, analyzed, related to petrophysical properties, and finally this relationship will be applied to the whole seismic survey to get reservoir properties within seismic resolution.

There are many types of seismic attributes. Four types will be used in this research. The four types are; amplitude statistics, complex trace statistics, sequence statistics, and spectral statistics. Attributes of the first three types will be used for quantitative interpretation of some reservoir properties such as porosity, water saturation and volume of silt. Moreover, a qualitative study will be made using spectral attributes of all of the four types to verify the results reached from the quantitative study.

Theoretically, it is difficult to derive a relationship between a seismic attribute and a physical property because such a relationship varies from one region to another. However, it is found that the simultaneous analysis of seismic attributes with borehole data leads to better estimates of reservoir properties than using only borehole data.

CHAPTER 2

Seismic Attributes

Seismic attributes are transformations of the seismic trace. They enable us to look at the amplitude information from different angles. In this research nine seismic attributes will be calculated to be analyzed and related to some reservoir properties. These attributes belong to three classes which are amplitude statistics, complex trace statistics, and sequence statistics. In addition to these three classes, spectral attributes will also be used to verify our interpretation qualitatively.

Amplitude Statistics

Average absolute amplitude, average peak amplitude, maximum peak amplitude, and RMS amplitude are the attributes to be used from the amplitude statistics class. Amplitude information can help in identifying gas and fluid accumulation, gross lithology, channel or deltaic sand, certain types of reefs, unconformities, tuning effect, and changing sequence stratigraphy.

RMS Amplitude

RMS (root mean square) amplitude is the square root of the average of the squares of the amplitudes calculated within a specific window.

$$RMS\ amplitude = \sqrt{\frac{1}{n}\sum_{i=1}^{n}(a_i)^2}$$

Where a_i is the amplitude of the i^{th} sample point.

Since the amplitudes are squared, the RMS amplitude is very sensitive to extreme amplitudes. This attribute is most useful in detecting lateral changes in amplitudes due to changes in lithology.

Within a smaller analysis window (50 -100 ms) or less, RMS amplitudes can detect amplitude anomalies due to gas and fluid accumulation, unconformities, or tuning effect.

Average Absolute Amplitude

It is the sum of the absolute amplitudes in a specific window divided by the number of samples.

$$Average\ Absolute\ Amplitude = \frac{\sum_{i=1}^{n}|a_i|}{n}$$

This attribute is useful in detecting lateral changes in sequence amplitude due to changing lithology. Within smaller windows, average absolute amplitude can detect anomalies similar to those detected by RMS amplitude.

While RMS amplitude may better identify specific amplitude anomalies, average absolute amplitude may better characterize sequence interval amplitudes (Brown,1987).

Maximum Peak Amplitude

It identifies the largest positive amplitude in the analysis window. Maximum peak amplitude is best used for mapping amplitude anomalies within sequences or along a specific reflector. Such anomalies may result from gas and fluid accumulations, unconformities, or tuning effects.

Average Peak Amplitude

It is the sum of positive amplitudes divided by the number of positive samples.

$$Average\ Peak\ Amplitude = \frac{\sum_{i=1}^{m} a_i}{m}$$

Where m = Number of positive samples

a_i = Positive amplitude at i^{th} sample point.

This attribute has similar uses as RMS amplitude, but it is most useful for detecting lateral changes in a sequence due to changing lithology.

Complex Trace Statistics

Average reflection strength, average instantaneous phase, average instantaneous frequency are the attributes going to be used from the complex trace class.

Complex trace statistics can help in identifying gas and fluid accumulations, gross lithology, channel and deltaic sands, certain types of reefs, unconformities, changing sequence stratigraphy, fracturing, and tuning effects.

Before being able to calculate the attributes Hilbert transform need to be performed firstly to get the imaginary component of the complex trace (Taner, 1994).

$$F(t) = f(t) + ih(t)$$

Where f(t) is the real component (observed seismic trace),

h(t) is the imaginary component (quadrature trace).

The imaginary component h(t) is determined from f(t) using Hilbert transform,

$$h(t) = \frac{1}{\pi t} * f(t)$$

Where;* denotes deconvolution.

So, the complex trace can be written as

$$F(t) = f(t) + ih(t)$$

$$= A(t)\cos\theta(t) + iA(t)\sin\theta(t)$$

$$= A(t)\, e^{i\theta(t)}$$

Where A(t) is a time dependent amplitude,

$\theta(t)$ is a time dependent phase.

Average Reflection Strength

It is the envelope of a seismic trace or modulus of the complex function.

$$Average\ Reflection\ Stregth = \sqrt{f^2(t) + h^2(t)}$$

This attribute has a similar use as amplitude statistics, but it is more sensitive to amplitude anomalies because amplitude information is isolated from phase information. It is very useful in detecting changes in sequence amplitudes due to changes in lithology, and in identifying amplitude anomalies due to gas and fluid accumulations, unconformities, and tuning effects.

Average Instantaneous phase

It describes the angle between the vector formed by the real and imaginary components of the complex trace and the real axis as a function of time.

$$\theta(t) = \text{atan}\left(\frac{h(t)}{f(t)}\right)$$

It gives information about the overall phase characteristics of a seismic interval. Lateral changes in phase may explain the changes of fluid content of sediments or changes in bedding character of a specific event.

The instantaneous phase can help in deciding whether the amplitude changes found in one of the amplitude attributes are due to tuning, to hydrocarbon or to other effects.

Average Instantaneous Frequency

Instantaneous frequency is the rate of change of the instantaneous phase. It is obtained by taking the derivative of the instantaneous phase with respect to time (Taner, 1994).

$$Freq(t) = \frac{d}{dt}\theta(t) = \frac{d}{dt}\text{atan}\left(\frac{h(t)}{f(t)}\right)$$

It helps in locating areas of high porosity and rocks saturated with hydrocarbons because high frequencies will be attenuated more under the above conditions. Spectral attributes should be looked at in conjunction with this attribute to verify anomalies (as will be shown in Chapter 4).

Sequence Statistics

This class focuses upon energy buildup in a sequence and in polarity comparisons. Sequence statistics can help in identifying lithologic sequences, mapping sequence stratigraphy and characterizing certain amplitude anomalies.

Energy Half-Time

Energy half-time is a measure of the time required for the energy within a specified window to reach half its eventual total.

For constant amplitudes within a window, energy half-time will be at the center of the window. For stronger amplitude in the shallower part, the energy half time will take less time to reach half the total energy. For stronger amplitudes at the deeper part of the interval, the energy half time will take longer to reach half the total energy.

Let

$$Total\ Energy = \sum_{i=1}^{n} (a_i)^2$$

Where n= number of samples,

a_i= Amplitude at i^{th} sample.

Suppose for 1<m<n, we have

$$\sum_{i=1}^{m} a_i^2 = \frac{1}{2}\sum_{i=1}^{n} a_i^2$$

Then the energy distribution in a window is characterized by the m/n ratio which is 0.5 for uniform amplitudes within the window.

Energy half time can help in defining lateral changes in stratigraphy or amplitude anomalies associated with fluid content, unconformities, or changing lithology.

Positive to Negative Ratio

This attribute refers to the number of positive samples within the analysis window divided by the number of negative samples for each trace. Its variations may be correlated with stratigraphic changes. Also, thinning and thickening of sequences may be detected by this attribute (as will be shown in Chapter 4).

Spectral Statistics

Spectral statistics will only be used for qualitative interpretation of the data. The reason for not using it in the quantitative approach is that it needs a larger analysis window, greater than 40 msec, to be stable while the analysis window used to calculate the attributes for the quantitative study was around 30 msec. As a result, the analysis window is going to be enlarged to include the zone of interest and a part below it. The window will be 50 msec.

Suppose that the dominant frequency is 40 Hz. The period is 1/40 =0.025 sec. The program needs at least two full periods to determine the frequency, so at least 50 msec. window is needed.

The spectral statistics class offers means of characterizing the amplitude spectra of the seismic data. The amplitude (power) spectrum plot provides a good graphical representation of the individual frequency contributions to the seismic data.

Dominant frequency series, peak spectral frequency, and spectral slope from peak to maximum frequency are the attributes to be used. They provide information about the areas of fracturing, area of anomalous absorption due to the presence of gas, tuning effects, and wavelet characteristics as affected by overlying lithology.

Dominant Frequency Series

For a specified seismic interval, an estimate of the three most dominant frequency components of the power spectrum is made. Lateral changes in any or all of these frequencies mean that there may be gas saturation, fracturing, changing stratigraphy, or changing porosity.

The dominant frequency series provide information about the three most important points in the amplitude spectrum (Fig. 1).

Peak Spectral Frequency

Peak spectral frequency is similar to the dominant frequency components of the power spectrum, but it is an estimate of only the single most dominant frequency component. Peak spectral frequency attribute reflects changes in frequency characteristics which may be caused by hydrocarbon saturation, fracturing or changing lithology (Fig. 1).

Spectral Slope from Peak to Maximum Frequency

This attribute explains how high frequencies are absorbed within the analysis window. It is quantifying frequency absorption effects by estimating the decay of the amplitude spectrum(dB/Hz). Lateral changes of spectral slope may indicate absorption effects caused by gas saturation, fracturing, porosity changes, stratigraphic or lithologic changes (Fig. 1).

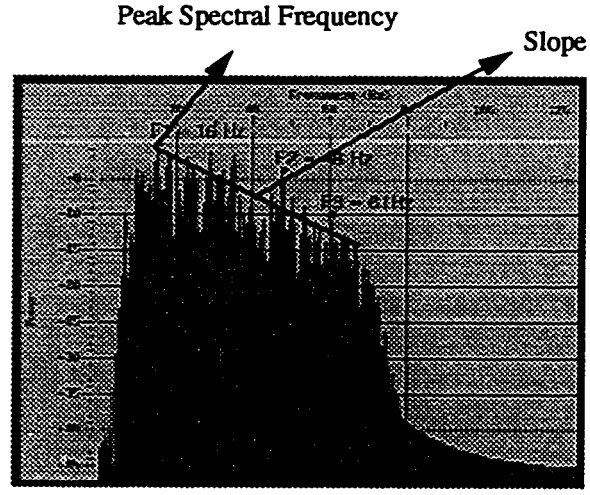

Figure 1: Spectral frequency attributes.

CHAPTER 3

Methodology

Previously, seismic data have only been used for structural interpretation. The amplitude character was totally destroyed during the processing phase in order to enhance the lateral continuity of seismic events. However, due to the demand for stratigraphic traps, the amplitude information becomes very important. Consequently seismic data have to be processed carefully to preserve the amplitude characteristics in order to use them to estimate reservoir properties using seismic data, well data, and geological information.

Seismic data which are going to be used for stratigraphic interpretation and reservoir property calculations must be processed in a way that the resulting seismic section has the highest quality, highest resolution, and widest band width (Taner, 1991).

To have seismic sections with the highest possible resolution, we have to understand the factors affecting resolution. The effect of seismic wavelets and processing sequences on the resolution of the seismic section need to be understood. It has been found that a wavelet with smooth and fast decaying envelope with only one peak at the center produces the desired resolution (Taner, 1991). Figure 2a shows that the zero phase Ricker wavelet with 30 Hz frequency is able to distinguish between the two layers while the minimum phase wavelet with the same frequency (Fig. 2b) can not distinguish between them.

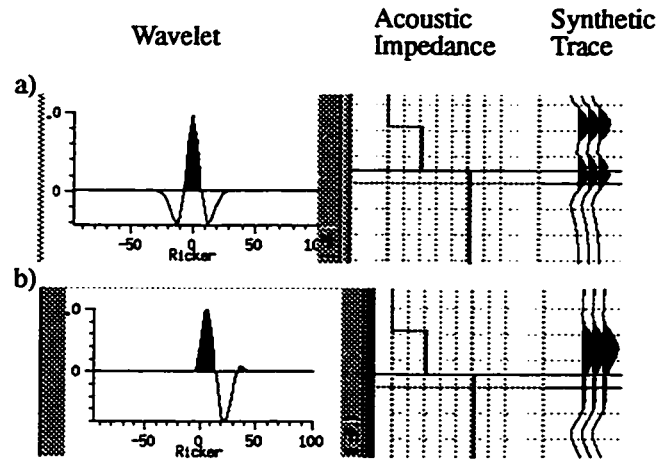

Figure 2: The effect of the wavelet shape on resolution. a) Zero phase Ricker wavelet used. b) Minimum phase wavelet used.

In addition to the resolution of seismic data, both amplitude and phase components must be considered and maintained during processing.

Stacking is one of the processes that affect the phase and the amplitude information severely. The primary events must be in phase in order to be stacked correctly. Otherwise, the stacked traces will contain events with arbitrary phase characteristics.

In a stratigraphic processing sequence, wavelet extraction and shaping should be applied to the common source and the common receiver traces, which will make the seismic data surface-consistent. After that, conventional refraction statics is sufficient to determine long-wavelength statics. Conventional velocity computation is reasonable in determining stacking velocities. Residual statics correction algorithm should compute time, amplitude, and phase-rotation residual statics, not only time statics like in conventional seismic processing. As a result, seismic traces belonging to one common depth point will have similar amplitudes, aligned envelopes, and aligned instantaneous phase components before stacking. Thereafter, the stacking process will not destroy amplitude and phase information.

All features of the properly processed seismic data must correspond to changes in lithological properties, so seismic attributes must be reflecting the physical proper-

ties of the layers. However, there are no clear relationships between seismic attributes and reservoir properties.

Is there a way to approximate the relationships between seismic attributes and reservoir properties? The answer is yes. There are different ways to use seismic attributes to estimate reservoir properties: Inversion of Seismic Data, Amplitude Versus Offset, and Seismic Attribute Analysis are some of the methods used to predict reservoir properties from seismic data.

It has been found that the use of seismic data in conjunction with well information leads to a better estimate of reservoir properties than using only well information. Figure 3 shows a simple kriging of porosity using only 20 control points out of 22 points available. Figure 4 is a simple kriging of porosity using all of the 22 wells available. Comparison between the two kriging results (Figs. 3, 4) shows that a simple kriging cannot provide a good approximation of the values of the neglected wells, well A and well I. However, the porosity estimated using 19 wells and the seismic attributes gave a good approximation of the porosity values in the neglected wells (Fig. 5). This method indicates that there is a low porosity zone around well A and a higher porosity zone around well I, which is in agreement with the porosities calculated using information from all 22 wells.

Computing reservoir properties from seismic attributes is not an easy task because the relation between them is not defined and it varies from area to area and even from layer to layer. One way to compute these reservoir properties is called the "multi-attribute-driven reservoir properties" method. In this approach, we calculate different attributes of the seismic data and the reservoir properties of interest from well logs. Then we fit a statistical regression function between seismic attributes and reservoir properties. This regression function can then be applied to the whole data set to get reservoir properties within seismic resolution.

There is an issue we need to consider here, which is the number of control points available. For a small number of control points (i.e. wells), the uncertainty of the relationship will be greater. In such situations attributes with physically justifiable relation should only be used (Kalkomey, 1997). Figure 6a shows the fitting function obtained using 3 wells which are black. The dim points were neglected in obtaining the function. Notice the high correlation coefficient (0.99). When all of the wells were used the resultant line fitting the points is totally different but it is more accurate than the above one (Fig. 6b), even though the correlation coefficient is only 0.48. Imagine the amount of error which would arise in using the first relationship to estimate the reservoir properties instead of the second one. Also, having a good

fit (high correlation coefficient) between small number of points does not necessarily mean that the relationship obtained is accurate.

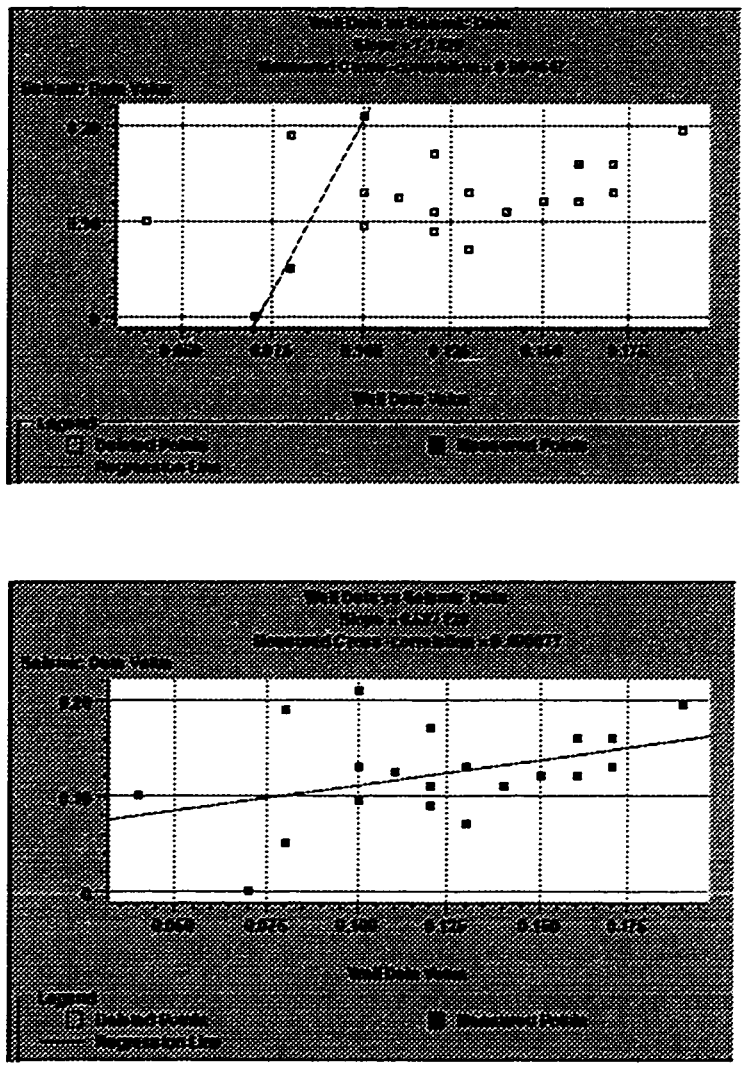

Figure 6: The uncertainty increases as the number of control points decreases. a) The line fitting three control points out of 21 points. b) The line fitting all of the 21 points.

In this research, nine seismic attributes were calculated and averaged on the reservoir interval, which is the interval between the Base Khuff Formation and the Pre Unayzah Unconformity (Fig. 7). After that, reservoir properties from 21 wells were averaged on the same interval. Nineteen of these wells were used for the analysis and the other two, well A and well I, were used for validating the results. The reservoir properties used are porosity, water saturation, and volume of silt. After that, seismic attributes near the wells were extracted and compared to the wells' reservoir properties. A relationship between seismic attributes and a given reservoir property was sought for in the form:

$$\sum_{j=1}^{m} W_j A_{ij} + C_i = L_i$$

where:

W= Weights,

A= Seismic attributes,

C= Constant,

L= Reservoir property,

i= Well number,

j= Attribute number.

To obtain this relationship, weights need to be assigned to attributes. To compute these weights, system of liner equations need to be solved.

$$\begin{bmatrix} 1 & A_{11} & A_{12} & \cdots & A_{1m} \\ 1 & A_{21} & A_{22} & \cdots & A_{2m} \\ | & & & & | \\ | & & & & | \\ 1 & A_{n1} & A_{n2} & \cdots & A_{nm} \end{bmatrix} \begin{bmatrix} C \\ w_1 \\ w_2 \\ | \\ w_m \end{bmatrix} = \begin{bmatrix} L_1 \\ L_2 \\ | \\ | \\ L_N \end{bmatrix}$$

Where;

C= Constant,

n= number of wells which is 19,

m= Number of attributes which is 9,

L= Reservoir property,

W= Weights,

A= Attribute values.

In the above system of equations, we have 10 unknowns and nineteen equations. Using multivariate regression analysis, we can get these unknowns and then apply the equations to the whole seismic data. In this project, a first degree polynomial was used to approximate reservoir properties. This function does not satisfy all of the wells fully. As a result the error need to be corrected. Differences between predicted porosities and original ones were calculated at well locations. The resultant differences were kriged. Then the resultant error map was added to the original porosity map.

The reason for using a first degree polynomial is to get a first approximation of reservoir properties and not to complicate results using a higher-order relationship. Higher-order relationships would fit the data points (19 wells) very well but they would also be affected by the noise in the data. However, a first-degree relationship acts as a low pass filter.

In some studies, neural networks failed to show reliable consistent results, though the relationship obtained fitted the data points very well (Yoshioka, 1996). I think the reason for this failure is that the relationship obtained was too complicated and mainly driven by the noise in the data.

The above results indicate that geological information combined with qualitative and quantitative interpretation of seismic attributes may lead to a successful prediction of the reservoir properties on the whole seismic survey.

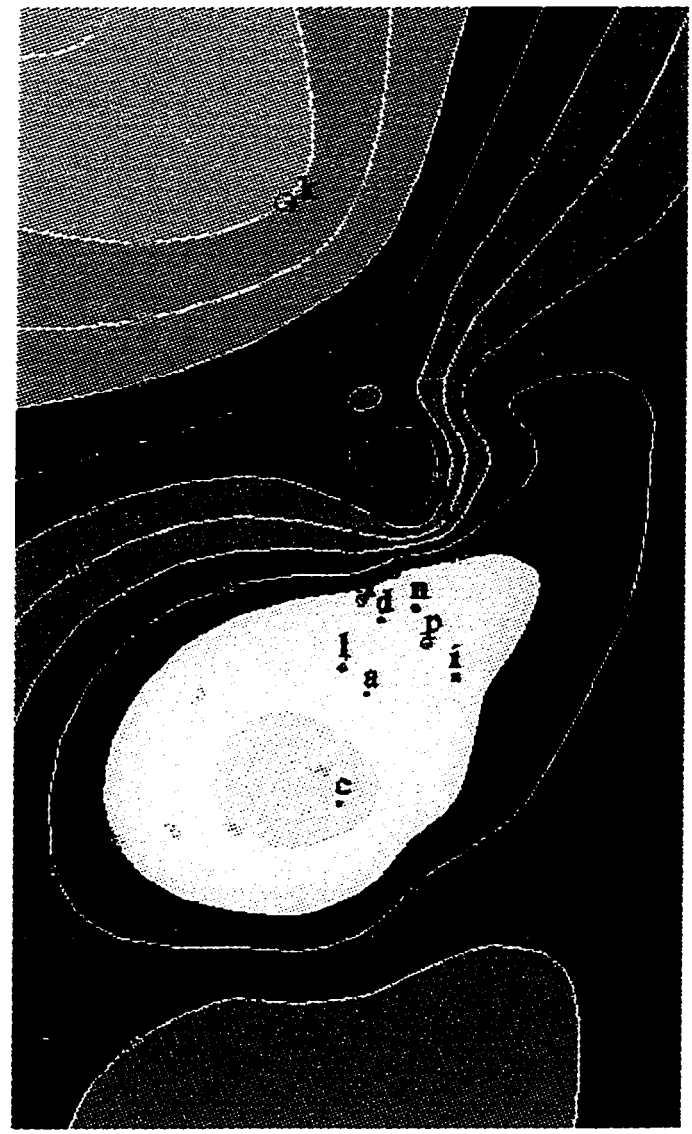

Figure 3: Porosity map generated using kriging of only well information. To generate this map 20 wells out of 22 were used (well A and well I were neglected).

Figure 4: Porosity map generated using kriging of only well information. To generate this map all of the wells were used.

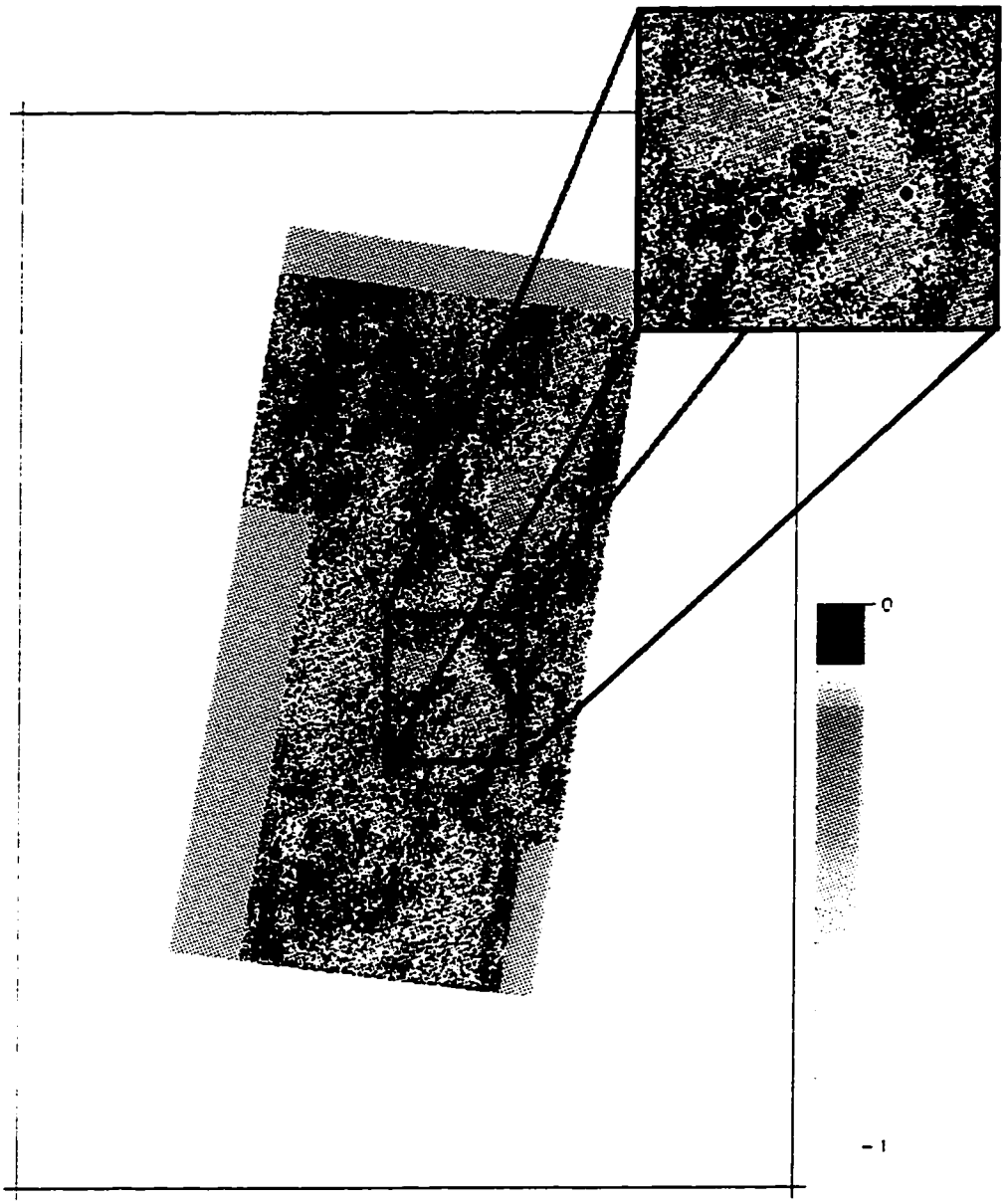

Figure 5: Porosity map generated showing the multi-attribute-driven porosity. To generate this map 19 wells out of 21 were used (well A and well I were neglected). Note that this method recognizes the difference between well A and well I without including them in the analysis. The variations between well A and well I can be seen in the zoomed version (upper right corner).

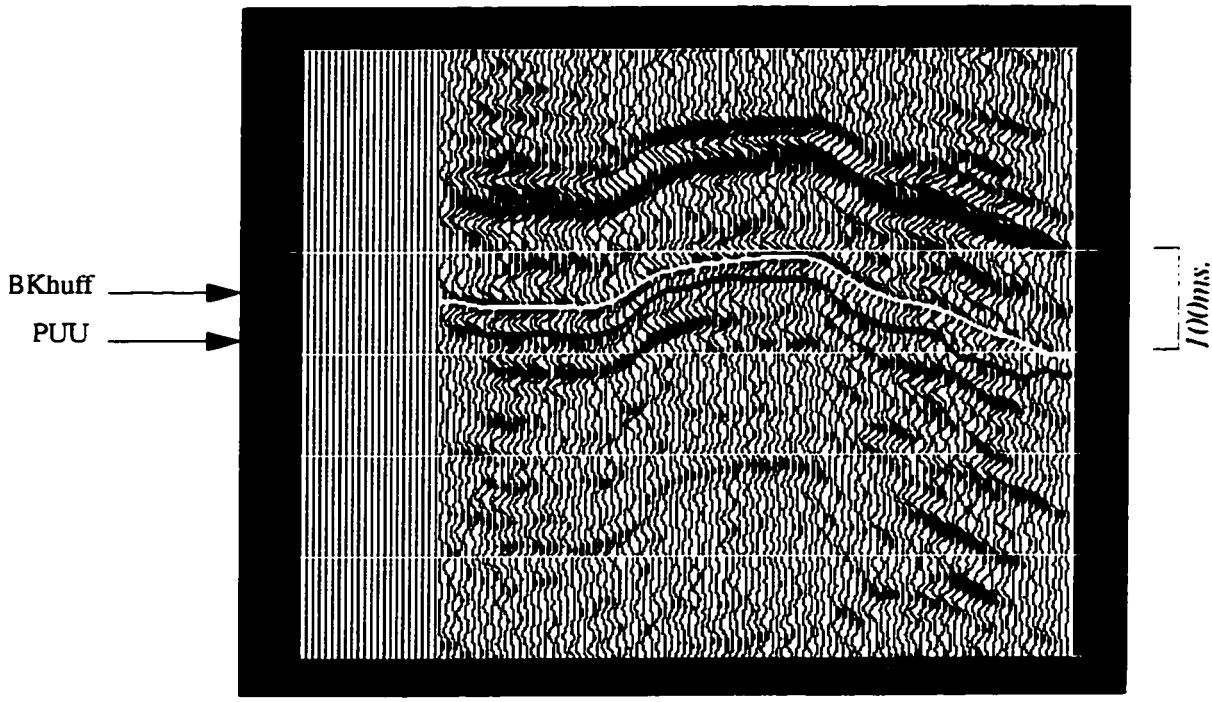

Figure 7: Seismic section with Base Khuff Formation and Pre Unayzah Unconformity shown.

CHAPTER 4

Application

The multi-attribute driven reservoir properties method was applied on a clastic reservoir. Attributes help in defining areas of good reservoir quality which can lead to a better understanding of the reservoir. The high spatial resolution of the resultant reservoir property maps increases the confidence for further interpretation of the reservoir.

The data used in this study belong to a producing field with lateral variations in reservoir properties. We proceed to map the variations of three reservoir properties using nine seismic attributes. The reservoir properties are porosity, volume of silt, and water saturation. The seismic attributes used are RMS amplitude, average absolute amplitude, maximum peak amplitude, average peak amplitude, average reflection strength, average instantaneous phase, average instantaneous frequency, energy half time, and positive to negative ratio. All attributes were scaled from 1 to 1000 in order to simplify the statistical analysis. In addition to the previous attributes, spectral attributes were calculated on a 50 msec. interval below the Base of Khuff Carbonate. The spectral attributes were used for qualitative interpretation because they need larger window than the one needed by the other nine attributes. As a result, spectral attributes cannot be used with the other attributes to calculate reservoir properties but they can help in the qualitative interpretation of the data (see Qualitative Interpretation Section, Chapter 5).

Seismic guidance in generating reservoir property maps is very important when a limited number of wells is available. As the number of wells increases, the importance of this method decreases but the accuracy increases.

Data Preparation

Three dimensional seismic data which had been processed stratigraphically to preserve relative amplitudes were used for the analysis. The data consisted of 277,536 traces. The survey contains 784 inlines and 354 crosslines with 50 X 50 meters spacing. The sampling rate is 2 msec.

The processing steps applied to the data were: Refraction statics to correct for long wavelength statics, velocity analysis, residual statics, surface consistent deconvolution, DMO, and poststack time migration. No automatic gain control was applied because this process distorts the amplitude information.

Attributes were calculated within the interval from Base Khuff Carbonate to Pre Unayzah Unconformity (Figs. 7, 8, 9). The thickness of this interval rangs from 11 to 50 msec. two way time (Fig. 10). Then these attributes were averaged on the same interval.

The reservoir properties were calculated from well logs and averaged on the same interval as the seismic data attributes in order to have a one-to-one comparison between them.

Geology of the Study Area

The Unayzah Formation consists of continentally deposited sandstones and siltstones. It is Early to Upper Permian in age and bounded by two major unconformities, Pre Khuff Unconformity at the top and Pre Unayzah (Hercynian) Unconformity at the bottom. The regional Unayzah section in the study area is divided into three major elements, upper sandstone, middle siltstone and lower sandstone. The lower sandstone which unconformably overlies the Qulaibah Formation (Silurian) is composed mainly of conglomerate and sandstone and it is called the Unayzah-B reservoir.

The lower part of Unayzah is interpreted as a braided channel-fill deposited sediments. The red siltstone separating the upper and lower sandstones is characterized by laminated gently dipping crossbeds and soft sediment deformation structures. It is interpreted as distal alluvial fan to playa deposited environment The uppermost Unayzah section is composed of fine-grained sandstone with very good reservoir quality that was deposited in fluvial environments as a stacked braided channel. This Unayzah section is called Unayzah-A reservoir (Fig. 11).

The Basal Khuff Clastics which unconformably overly the Unayzah Formation are present across the field with a reservoir quality development restricted to the north and south parts. No reservoir quality Basal Khuff Clastics are encountered in the central part of the field.

The Unayzah thickness ranges from 299 feet to 728 feet reflecting the paleotopography during the depositional processes. In general, the paleotopography was receiving most of the sediments through fluvial and gravity processes until all topographic relief came to be very gentle for the braided processes to take over and dominated the rest of Unayzah depositional system beside the eolian and playa lake deposits in the upper part of the section (Fig. 12). The main direction of the sedimentation processes is interpreted to be from nortwest to southeast (King, 1996).

The middle siltstone playa lake sediments were deposited mainly in the central part of the field with an average thickness of 100 feet and a maximum encountered thickness of 135 feet. This siltstone body of southwest-northeast trend is identifiable from the 3D seismic data and was confirmed by drilling.

The Unayzah Formation unconformably overlies many other formations of different rock types. Some of the overlain rocks are possible source rocks such as Jauf Carbonates, Jauf silts, and organic rich silt members of Qulaibah Formation. Moreover, the Unayzah Formation is overlain by Khuff Formation which is impermeable limestone and acts as a seal. The availability of the source rocks and the seal increases the probability of finding more reservoirs within the Unayzah Formation.

In addition to the source rock and the seal, the Unayzah Formation has porous zones in its lower and upper parts. The silt separating the lower and the upper good quality sands and the interdune, playa, lake margin sediments are of non-reservoir quality (King, 1996).

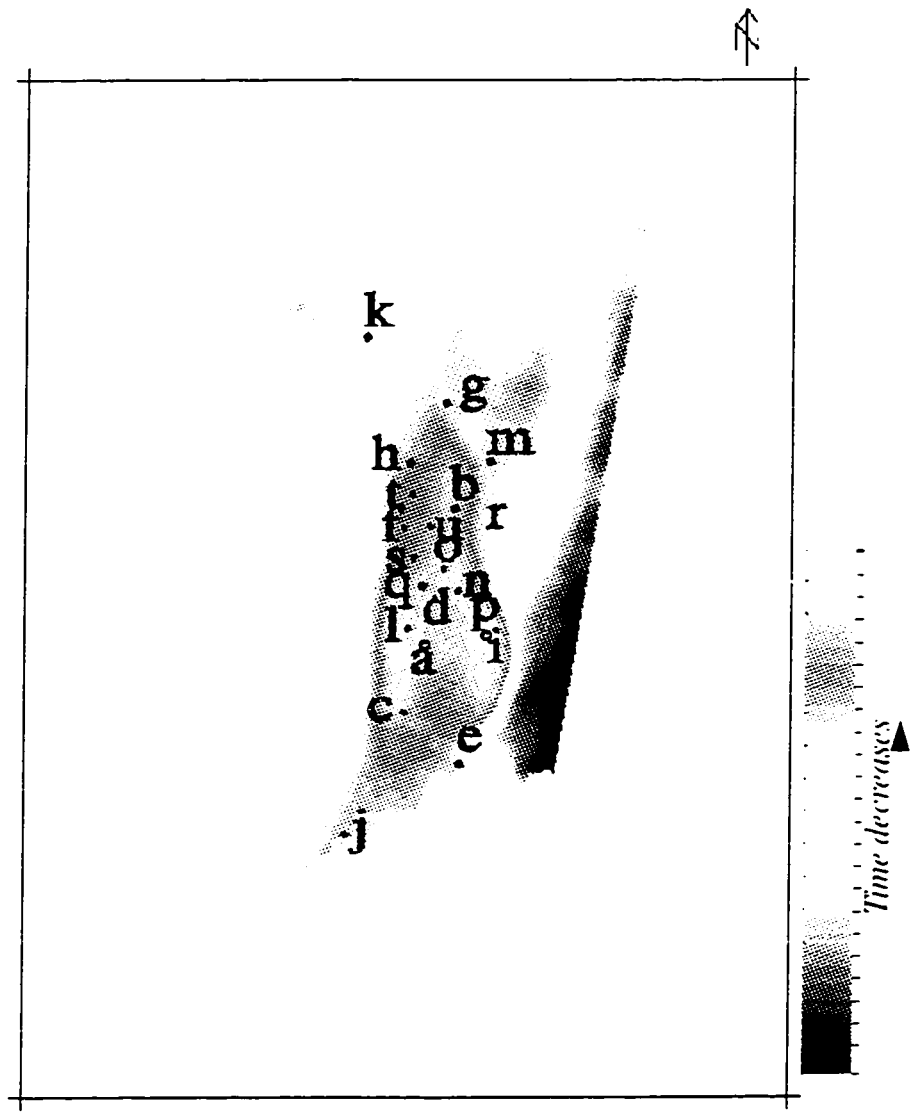

Figure 8: Map view of the Base Khuff Carbonate in two way travel time. The wells are posted. Red wells are the wells used in predicting reservoir properties. White wells are the neglected ones.

Figure 9: Map view of the Pre Unayzah Unconformity.

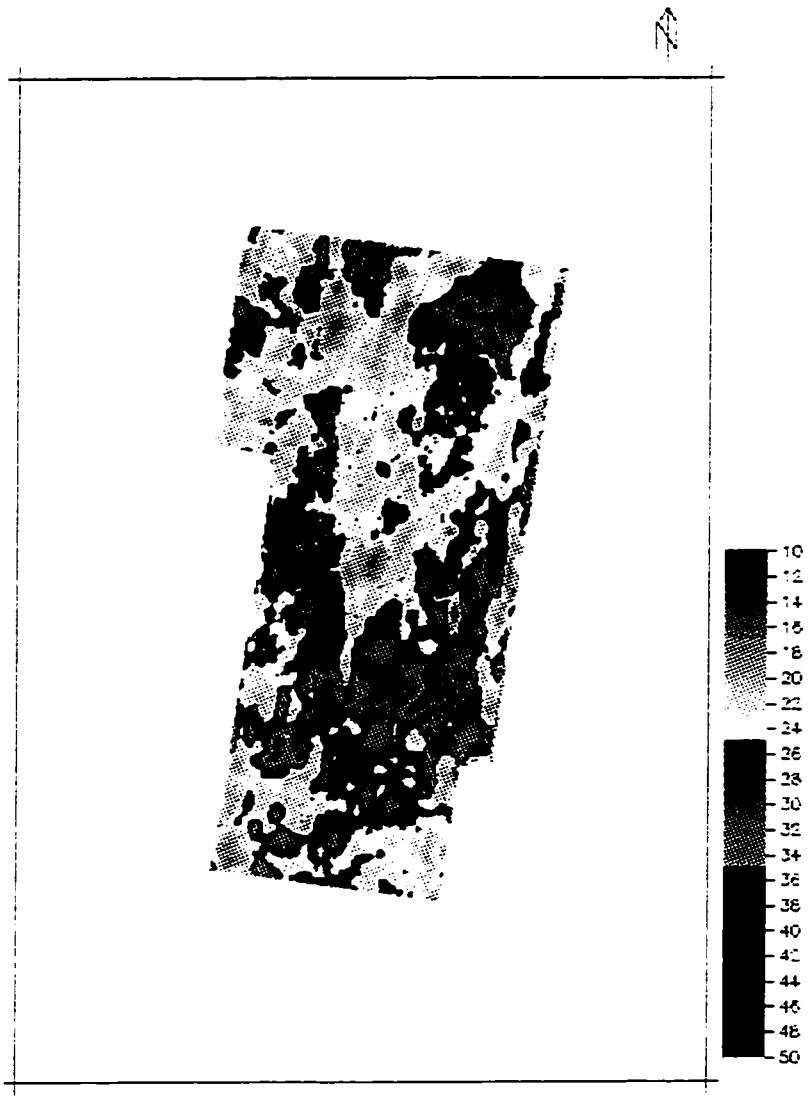

Figure 10: Map View of the time thickness of the interval between the Base Khuff Carbonate and the Pre Unayzah Unconformity.

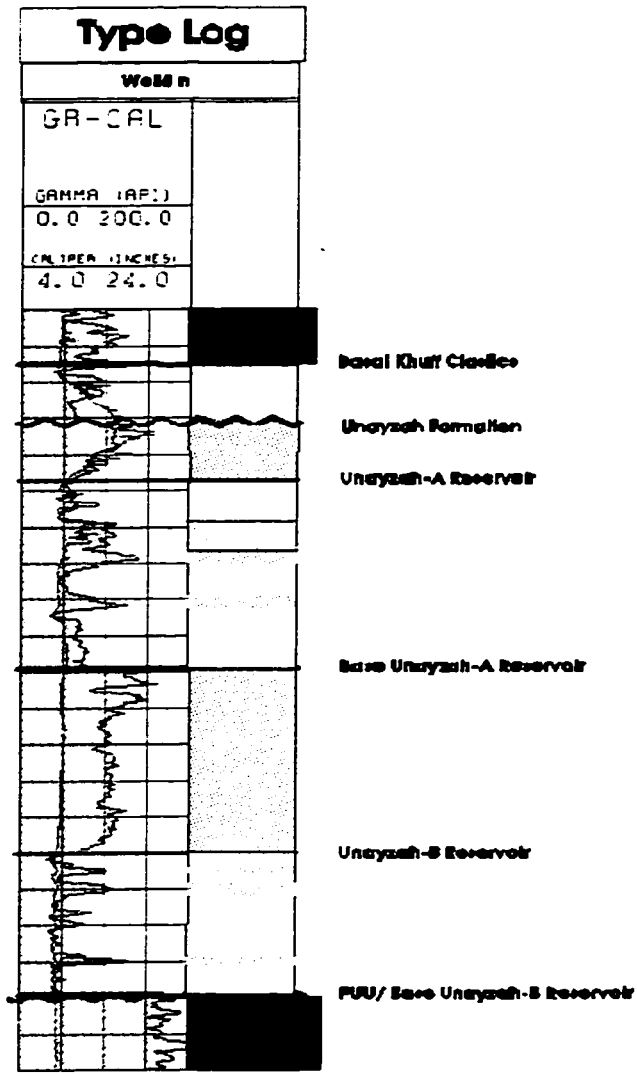

Figure 11: Gamma ray log and stratigraphic column showing the interval of interest.

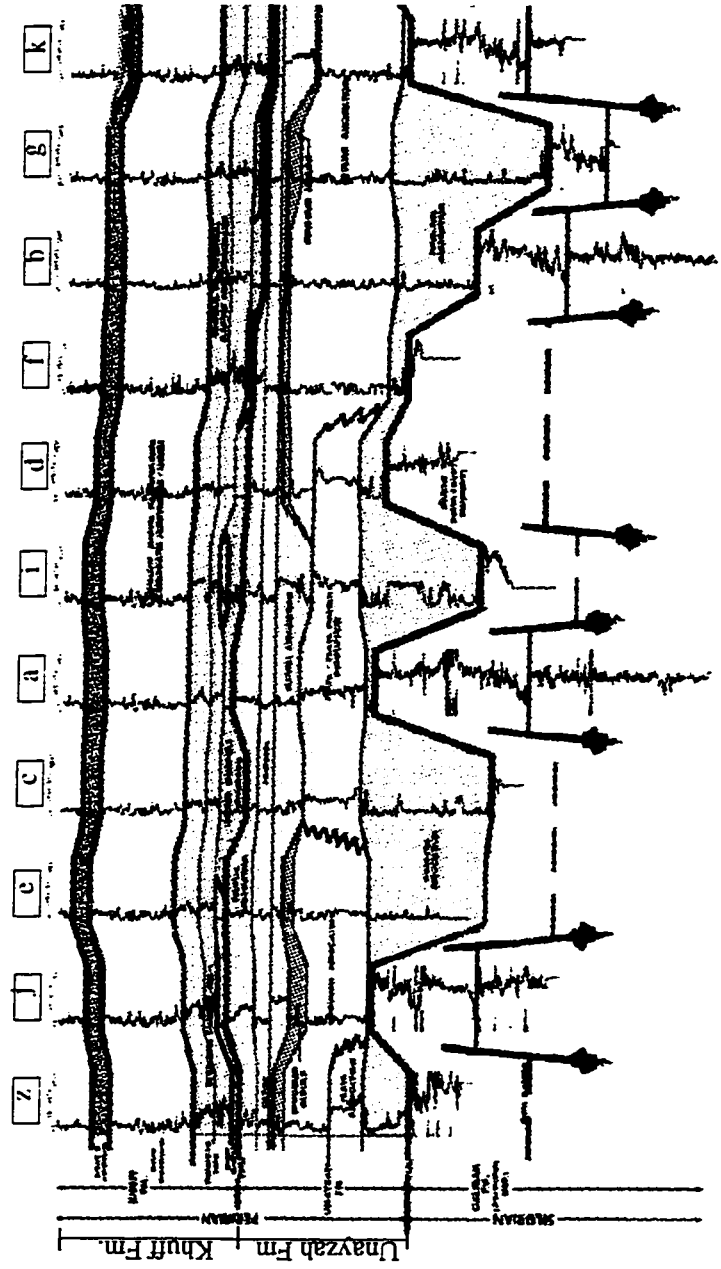

Figure 12: Stratigraphic cross section of the study area.

Data Analysis

The primary objective of this research is to produce reservoir property maps using multi-seismic attributes analysis. Three reservoir property maps were produced using nine seismic attributes. The reservoir property maps are porosity, water saturation, and volume of silt maps. The seismic attributes are: RMS amplitude (Fig. 13), average absolute amplitude (Fig. 14), maximum peak amplitude (Fig. 15), average peak amplitude (Fig. 16), average reflection strength (Fig. 17), average instantaneous phase (Fig. 18), average instantaneous frequency (Fig. 19), energy half-time (Fig. 20), and positive to negative ratio (Fig. 21).

All of the above seismic attributes were calculated and averaged on the interval from Base Khuff Carbonate to Pre Unayzah Unconformity (Figs. 6, 8, 9, Table 1, 2). The reservoir properties from 21 well logs were calculated and averaged on the same interval (Fig. 11, Table 3). Only nineteen wells were used to calculate reservoir property maps and the other two wells were kept to validate the method.

TABLE 1. Seismic attributes of the trace nearest to the well calculated and averaged on the interval from B-Khuff to PUU.

Well	Abs.Amp.	Ins.Freq.	Ins.Phase	PeakAmp.	Ref.Str.
B	524.55988	302.42776	632.46698	555.87451	531.43268
C	262.70132	244.84137	615.0119	158.34239	242.52849
D	322.56195	399.48236	624.44537	296.31406	326.49899
E	452.01831	309.97452	571.22473	318.24045	505.54221
F	604.28784	364.16064	545.9892	553.84143	609.75232
G	373.20172	305.58762	507.73434	381.9357	384.42142
H	253.93846	316.12082	606.09833	261.47354	249.38805
J	191.86037	424.452	511.42465	140.50558	203.58636
K	182.25285	508.40991	551.12878	197.61191	166.74879
L	461.67517	376.20184	528.93903	571.45221	448.8541
M	609.43707	362.97675	538.46228	568.03003	582.28772
N	331.93661	357.44763	544.29626	416.30661	346.39807
O	363.20651	332.82373	604.44043	471.5282	336.13812
P	382.87866	323.9212	607.37549	394.68253	367.04041

TABLE 1. Seismic attributes of the trace nearest to the well calculated and averaged on the interval from B-Khuff to PUU.

Well	Abs.Amp.	Ins.Freq.	Ins.Phase	PeakAmp.	Ref.Str.
Q	376.84119	309.28909	728.44836	439.3494	339.34003
R	534.6203	355.0986	609.48975	453.61807	525.18347
S	334.77374	390.96246	654.5097	404.56784	302.40894
T	485.89539	371.1601	562.37274	404.09613	523.21844
U	535.74805	353.30844	530.51697	441.20334	539.651

TABLE 2. Continuation of Table 1.

Well	Energy Half Time	Max Peak Amp.	RMS Amp.	Pos/Neg
B	487.01297	581.83826	516.88513	23.4375
C	803.57141	197.8864	266.49457	80.35714
D	194.80519	409.85989	334.40097	52.083332
E	576.9231	347.73657	475.82242	27.777779
F	625	511.22903	605.09479	31.25
G	446.42859	390.40555	372.62088	20.833334
H	194.80519	311.91162	252.31656	35.714287
J	389.61038	230.63652	199.99086	52.083332
K	357.14285	236.27873	186.45134	87.5
L	89.285713	660.03186	506.39621	44.642857
M	535.71429	542.875	594.13831	31.25
N	389.61038	428.16565	345.57025	23.4375
O	97.402596	453.49081	381.06046	52.083332
P	178.57143	478.29791	388.70566	44.642857
Q	119.04762	532.83447	436.47455	125
R	584.41559	489.1218	520.64758	35.714287
S	194.80519	363.96597	343.67484	75
T	487.01297	566.97949	500.45273	35.714287
U	625	466.00983	536.72278	44.642857

TABLE 3. Reservoir properties calculated and averaged from processed logs on the interval from B-Khuff to PUU.

Well	W.SAT.	POR.	V.SH.
A	0.83	0.04	0.66
B	0.64	0.17	0.09
C	0.91	0.08	0.36
D	0.71	0.08	0.46
E	0.99	0.12	0.18
F	0.64	0.13	0.13
G	0.87	0.16	0.07
H	0.75	0.15	0.10
I	0.74	0.10	0.16
J	0.73	0.13	0.28
K	0.88	0.19	0.19
L	0.62	0.10	0.17
M	0.92	0.13	0.11
N	0.63	0.10	0.12
O	0.61	0.11	0.14
P	0.53	0.12	0.12
Q	0.60	0.12	0.19
R	0.88	0.14	0.12
S	0.55	0.12	0.12
T	0.68	0.16	0.10
U	0.52	0.17	0.10

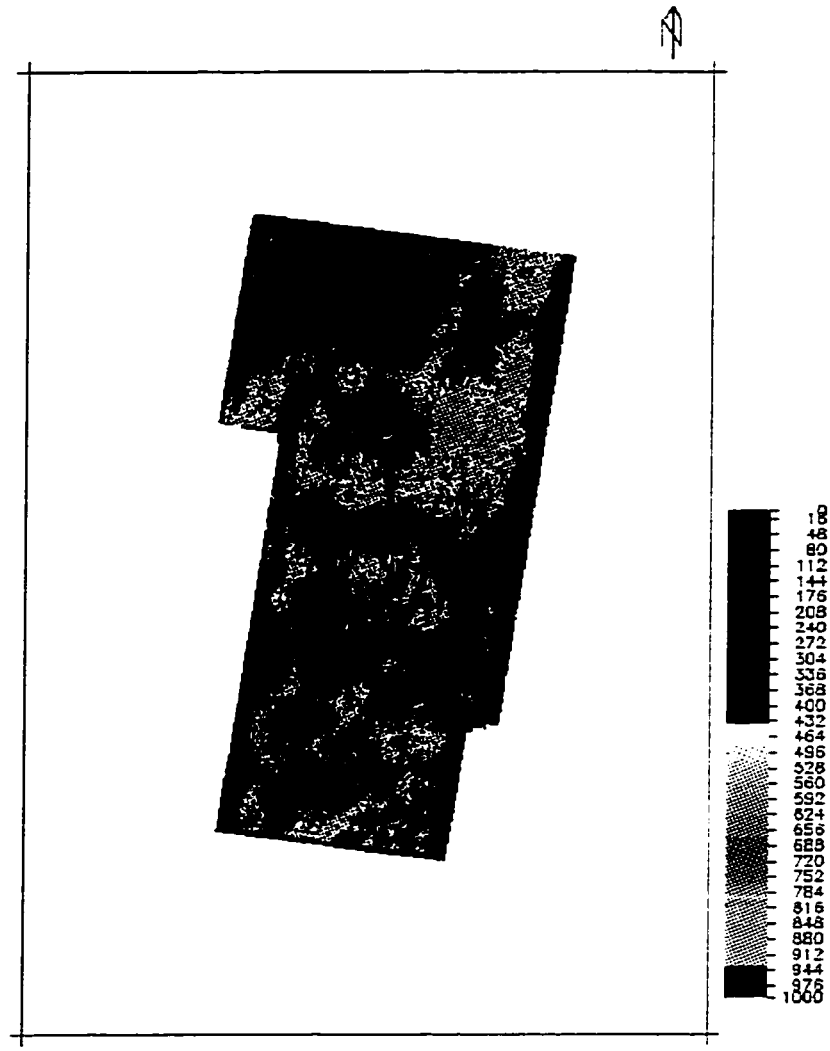

Figure 13: Root Mean Square amplitude attribute calculated and averaged over the interval of interest (B-Khuff to PUU).

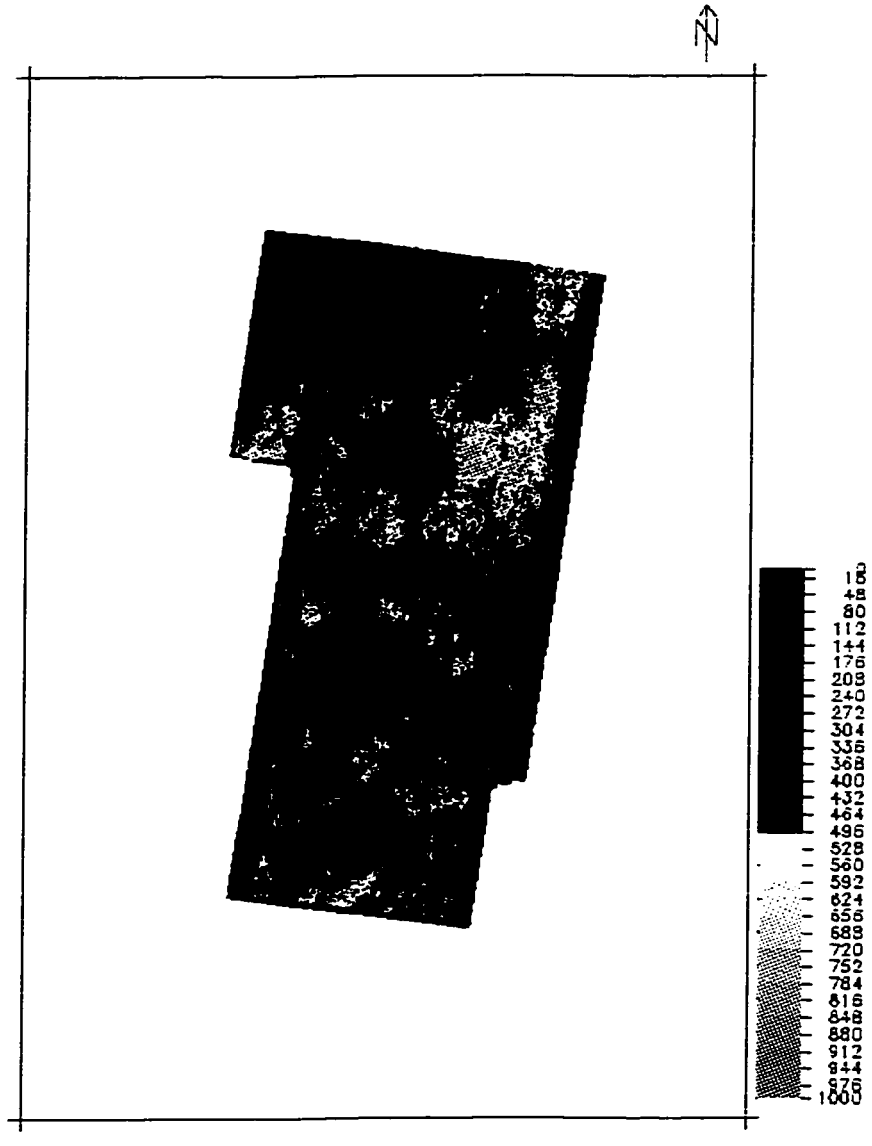

Figure 14: Average absolute amplitude calculated in the interval from Base Khuff to Pre Unayzah Unconformity.

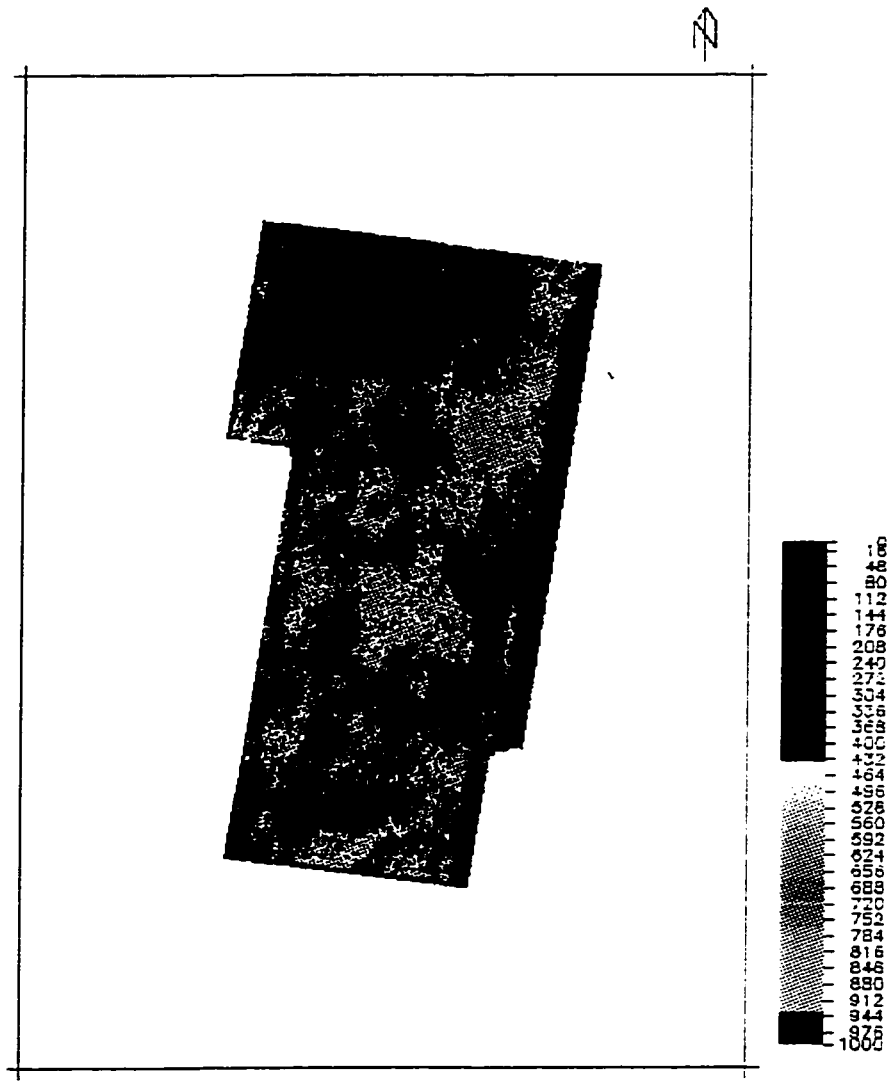

Figure 15: Maximum peak amplitude attribute calculated and averaged over the interval of interest.

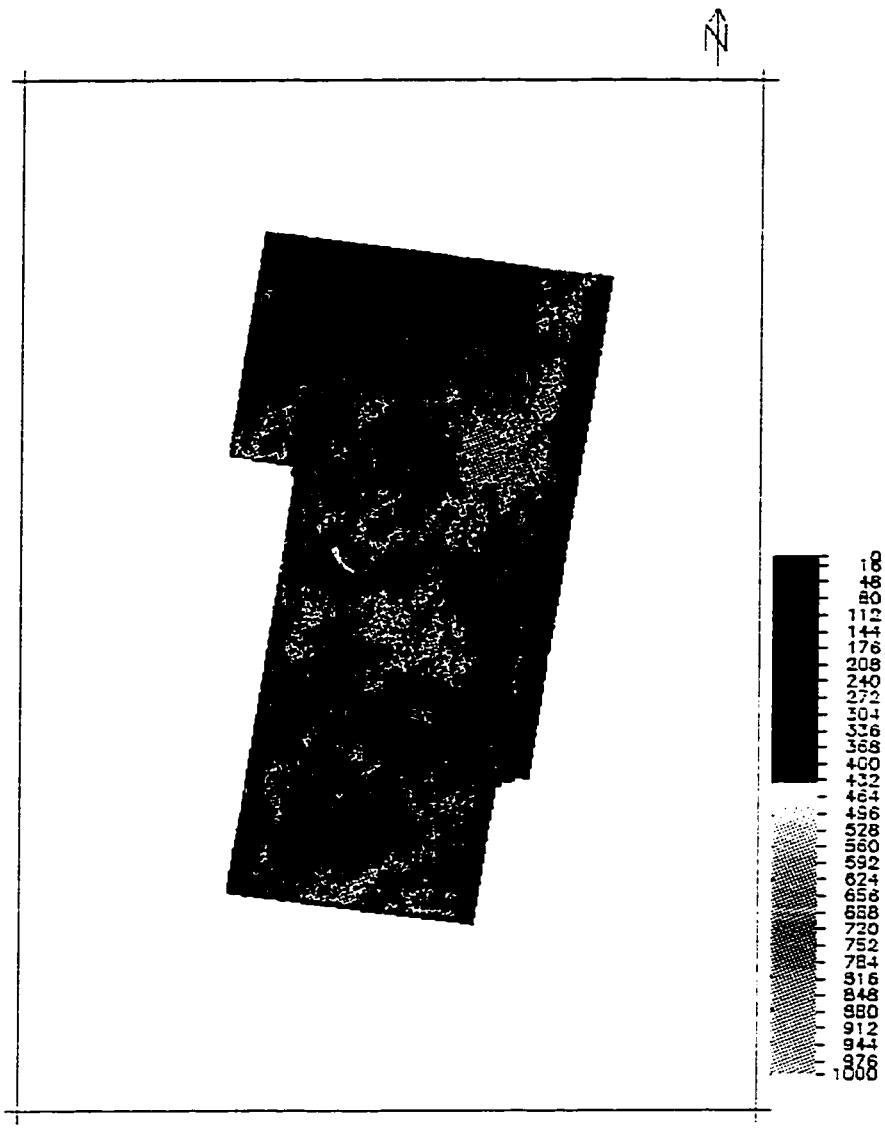

Figure 16: Average peak amplitude attribute calculated within the interval of interest.

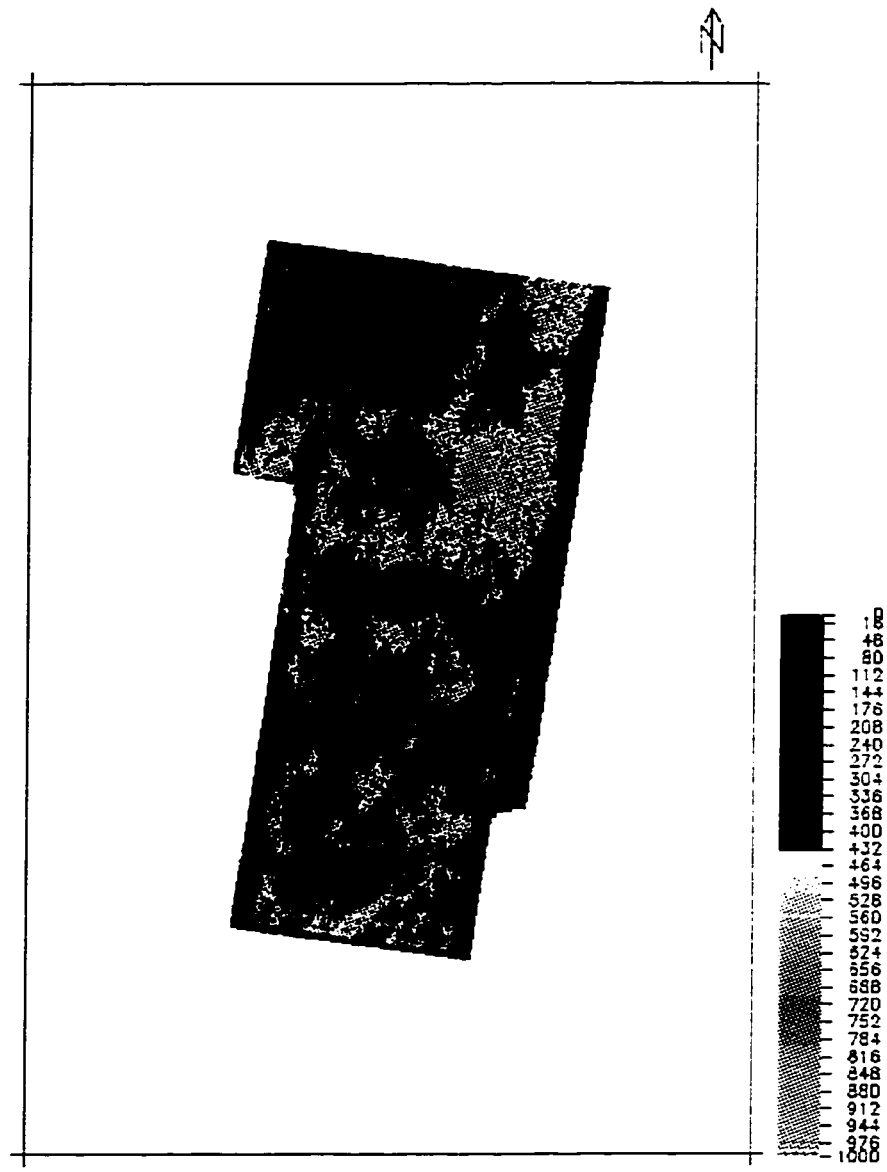

Figure 17: Reflection strength attribute calculated and averaged over the interval of interest.

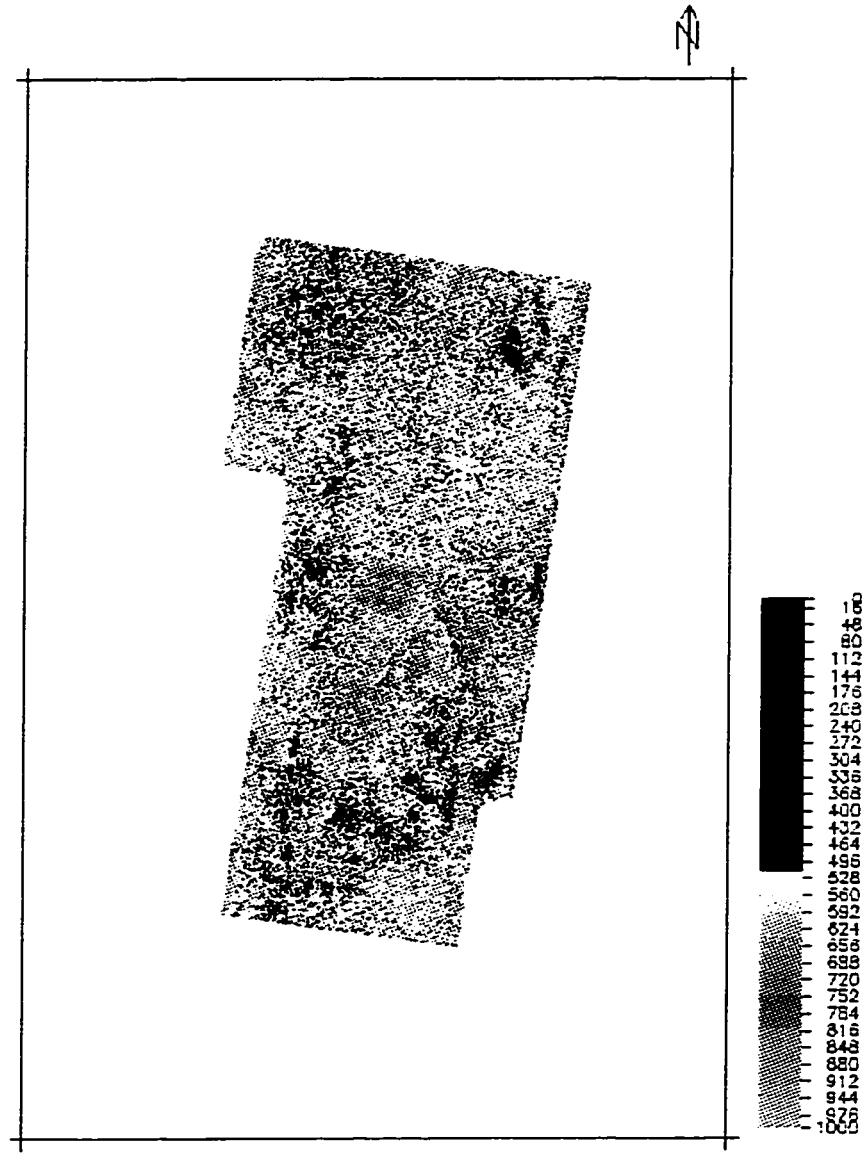

Figure 18: Instantaneous phase attribute calculated and averaged over the interval of interest.

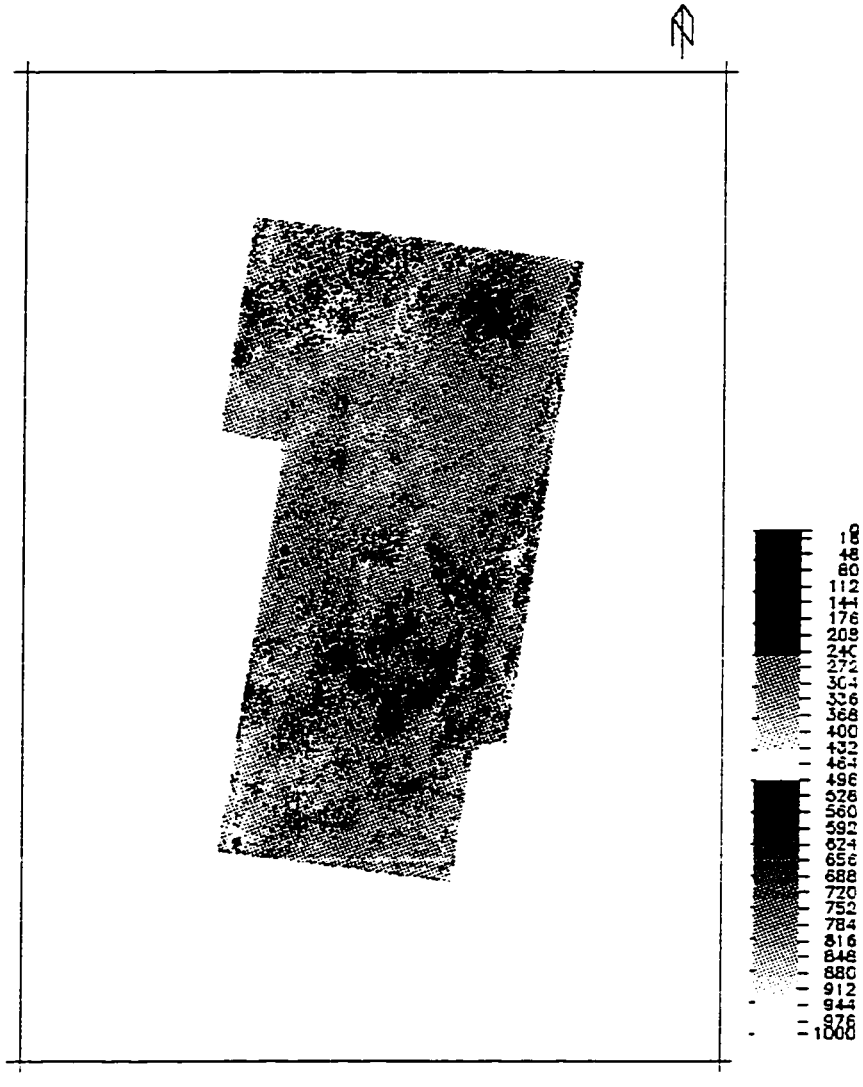

Figure 19:Instantaneous frequency attribute calculated and averaged over the interval of interest.

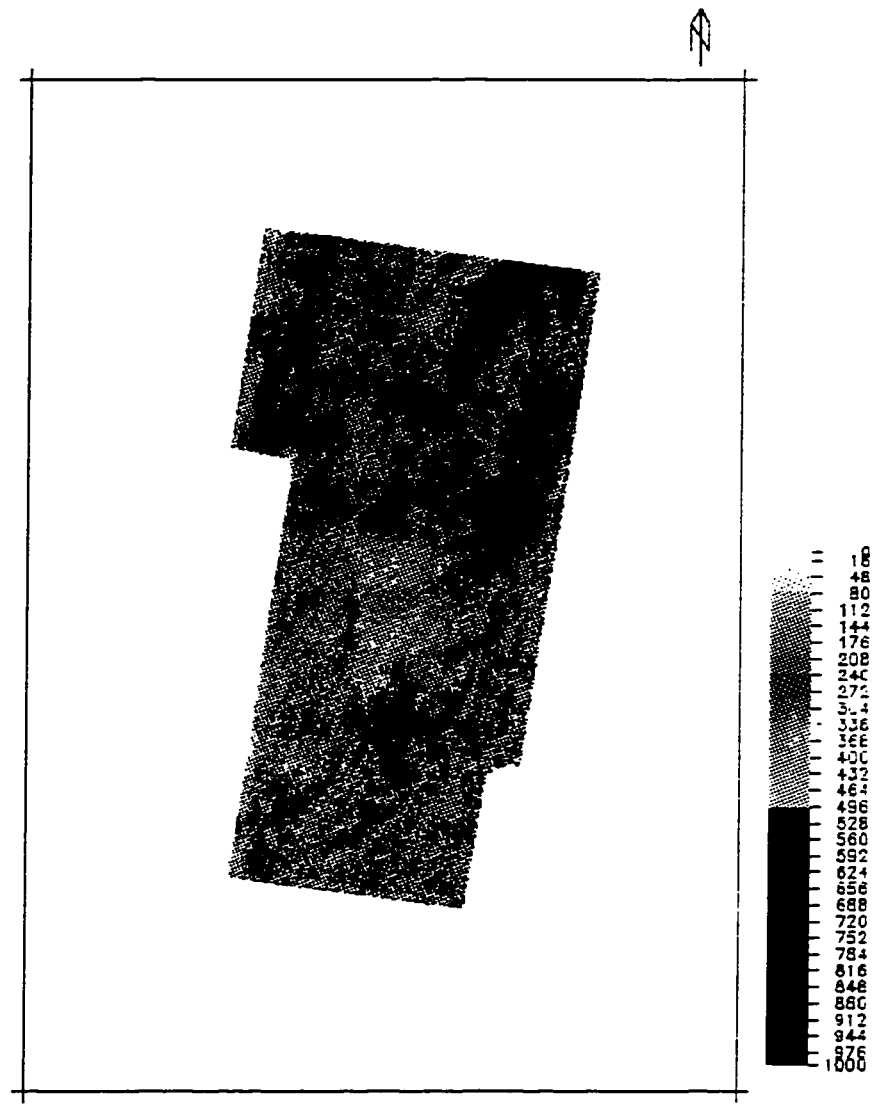

Figure 20:Energy half time attribute calculated and averaged over the interval of interest.

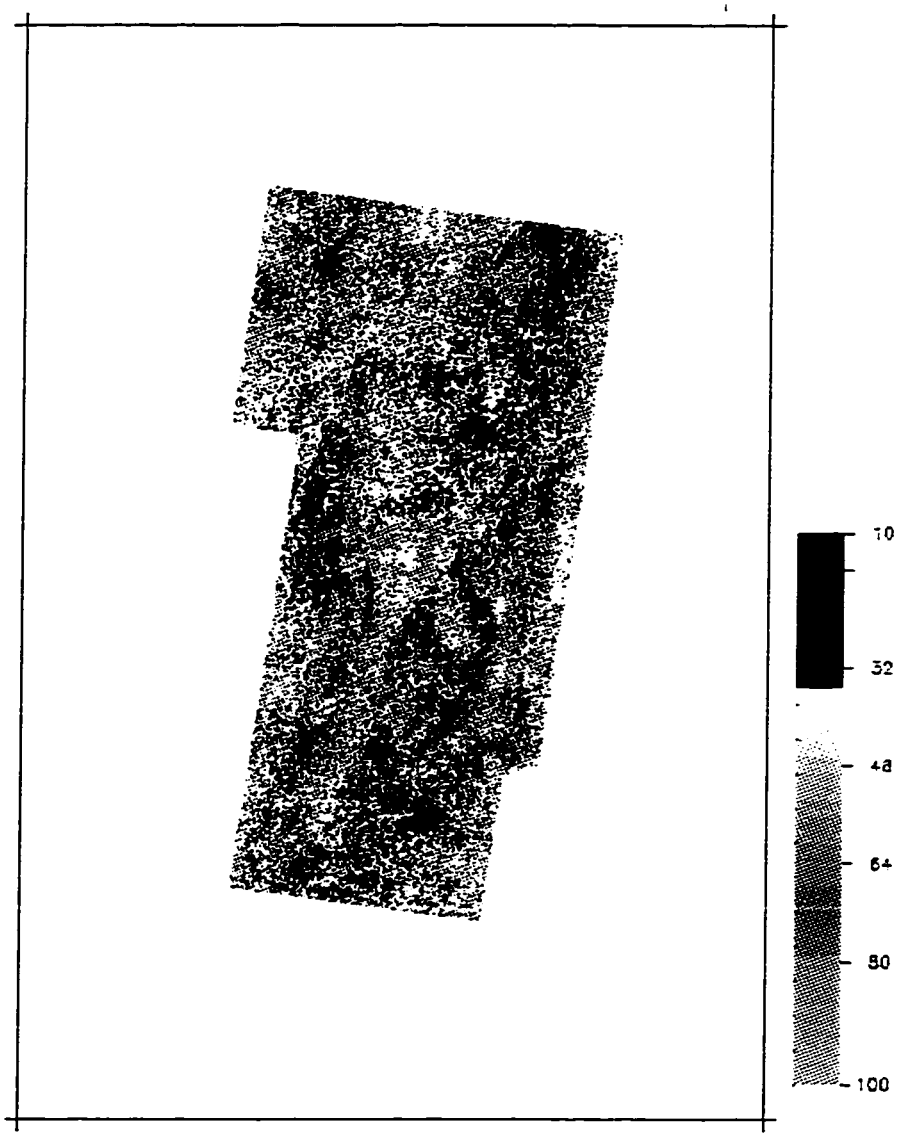

Figure 21: Positive to negative ratio attribute calculated and averaged over the interval of interest.

Weights were assigned to the nine seismic attributes in order to best predict the values of the reservoir properties at well locations using multivariate regression analysis.

$$L_i=W_1A_{1i}+W_2A_{2i}+W_3A_{3i}+.....+W_nA_{ni}+C_i$$

The weights obtained, using only 19 wells out of 21 wells, for predicting reservoir properties are shown in Table 4.

TABLE 4. Weights obtained for each seismic attribute.

	Dependent Variable		
Variable	**POR.**	**W.SAT.**	**V.SH.**
INTERCEPT	0.471922	0.419519	-0.812037
ABSAMP	0.001078	-0.000456	-0.001549
IFREQ	-0.000432	0.000748	0.001389
IPHASE	-0.000667	0.000677	0.001561
PEKAMP	0.000414	-0.000996	-0.001632
REFSTR	0.003142	-0.004075	-0.006407
ENHLFT	-0.000182	0.000395	0.000452
MAXPAMP	0.00005221	-0.000454	0.000326
RMSAMP	-0.004373	0.005244	0.008391
POSNEGR	0.004060	-0.005614	-0.007652

Reflection strength, RMS amplitude and positive to negative ratios were given high weights relative to the other attributes. This means that these three attributes have the highest effect on reservoir properties calculations.

Using weights of all attributes, reservoir properties of the traces nearest to the wells were calculated first and compared with the original reservoir properties. For example, to calculate the porosity at the trace nearest to well_B, we need to use weights from Table 4 and apply them to the seismic attributes (Tables 1,2). The resultant relation well be as follows:

$$\text{Calculated Porosity}= W_1A_1+W_2A_2+W_3A_3+..... +W_9A_9 +C$$

=0.001078*524.560-0.000432*302.428-0.000667*632.467+0.000414*555.875+
0.003142*531.433-0.0001820*487.013+0.000052206*581.838-
0.004373*516.885+.004060*23.438+0.471922=0.1616

The original porosity value derived from the logs of well B is 0.17 which means that there is an error of 0.00839. Since we are fitting a linear relationship between attributes and reservoir properties, the function cannot honor all points. There will always be residuals (Figs. 22, 23, 24). As the next step, the obtained relationships were applied to the whole seismic survey in order to estimate porosity, water saturation, and volume of silt over the whole site (Figs. 5, 25, 26). These maps have high lateral resolution which means a better confidence in interpreting the reservoir.

As mentioned before, well A and well I were not used in the regression analysis and the generation of any of the three reservoir property maps. However, the predicted reservoir properties agree with the original properties for these two wells. The seismic multi-attributes-driven porosity map shows that well I has a higher porosity than well A while simple kriging of the well data could not predict the differences (Figs. 5, 3).

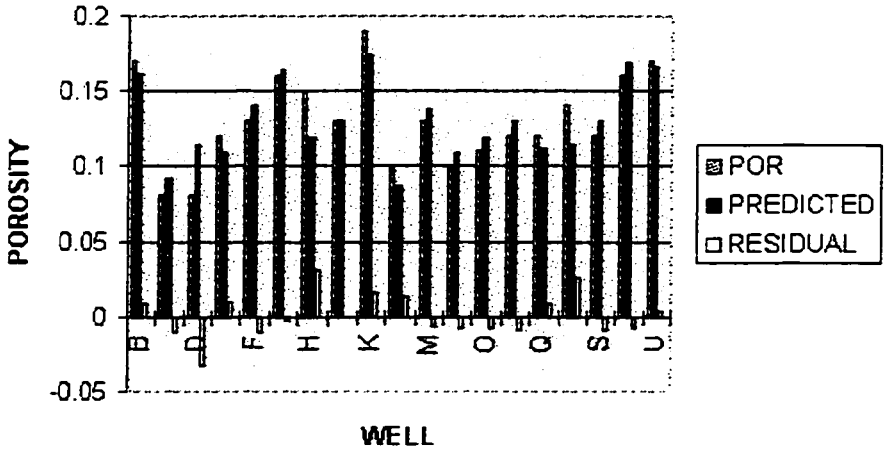

Figure 22: Original, predicted, and residuals of porosities at each well used in the analysis.

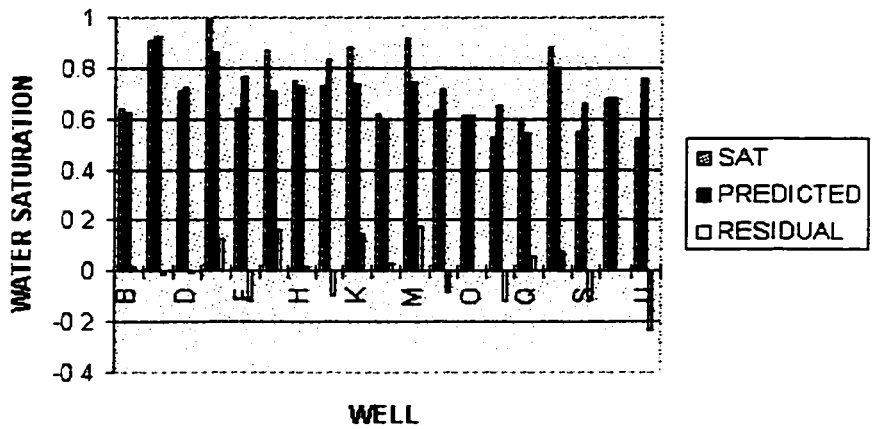

Figure 23: Original, predicted, and residuals of water saturations at each well used in the analysis.

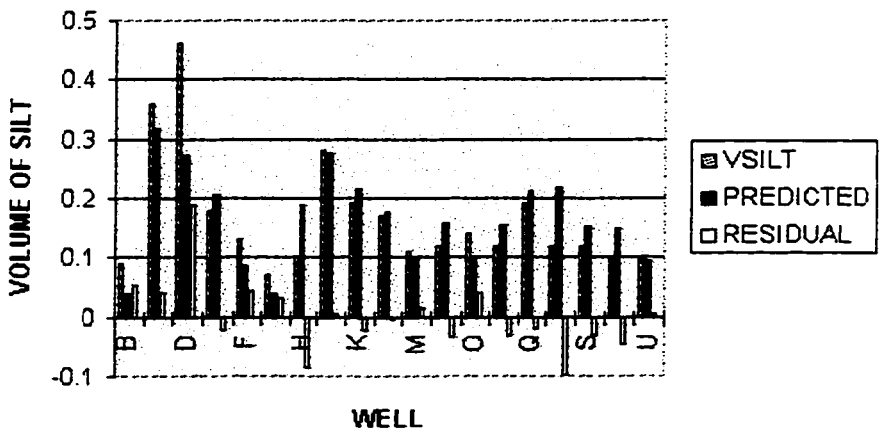

Figure 24: Original, predicted, and residuals of volume of silt values at each well used in the analysis.

The water saturation map (Fig. 25) shows higher water saturation at well A than at well I which agrees with the original water saturation values at these two well locations. Moreover, the volume of silt map (Fig. 26) shows higher values at well A than at well I which again agrees with the original log information.

The porosity map (Fig. 5) indicates that there is a trend of high porosities in the NNE-SSW direction. The lithology is not uniform in this reservoir interval as explained in the Geology of the Study Area section. The amount of variations in the porosities makes it very difficult to model the reservoir properties using only well information.

The water saturation map shows similar trend as the porosity map. Water saturations less than 0.7 follow NNE-SSW trend. This trend is surrounded by values greater than 0.7. Having lower water saturations with higher porosities increases the probability of hydrocarbon accumulations.

The volume of silt map shows similar trend for the values less than 0.1, and these points are surrounded by higher percentages of silt.

Combining the three maps, we identified a NNE-SSW trend having high porosity (greater than 0.1), low water saturation (less than 0.7), and low volume of silt (less than 0.1). This area is hopefully a clean sandstone with good porosity, permeability and hydrocarbon saturation.

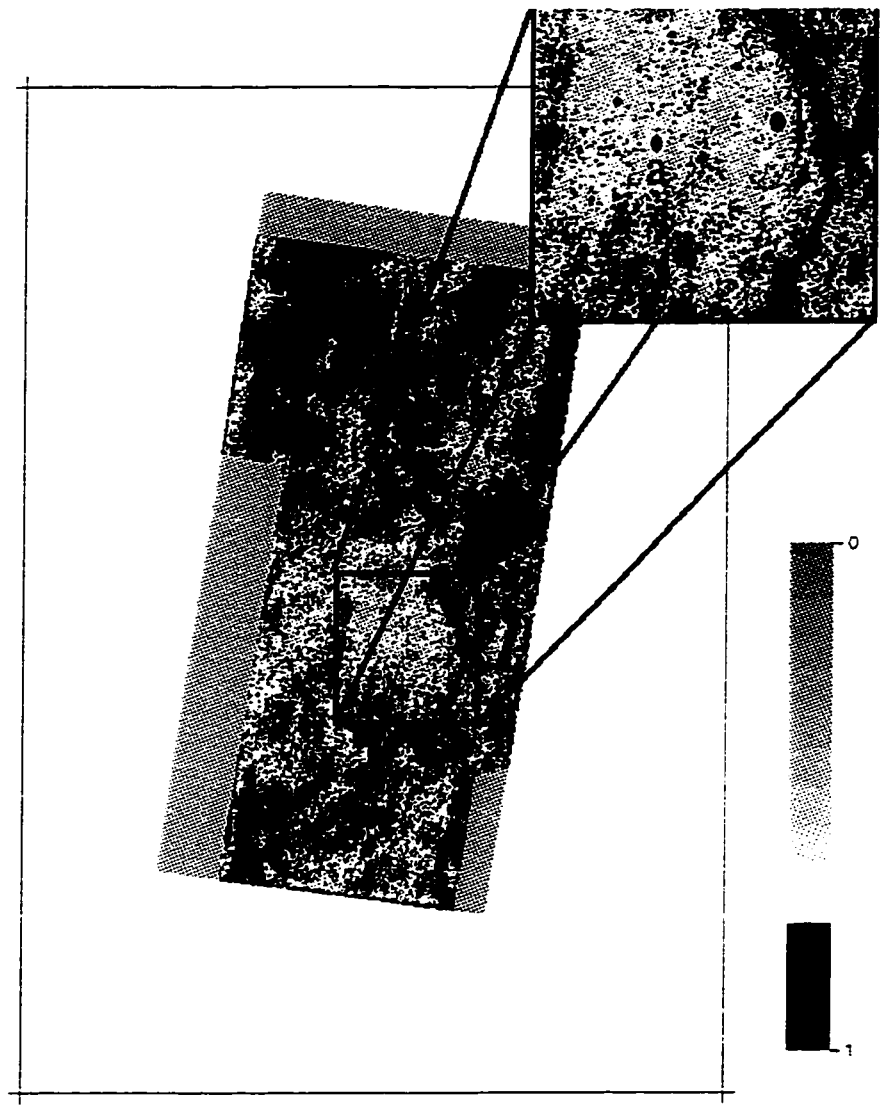

Figure 25:Water saturation map generated showing the multi-attribute driven water saturation. To generate this map19 wells out of 21 wells were used (well A and well I were neglected). Note that this method recognizes the difference between well A and well I without including them in the analysis. The variations between well A and well I can be seen in the zoomed version (upper right corner).

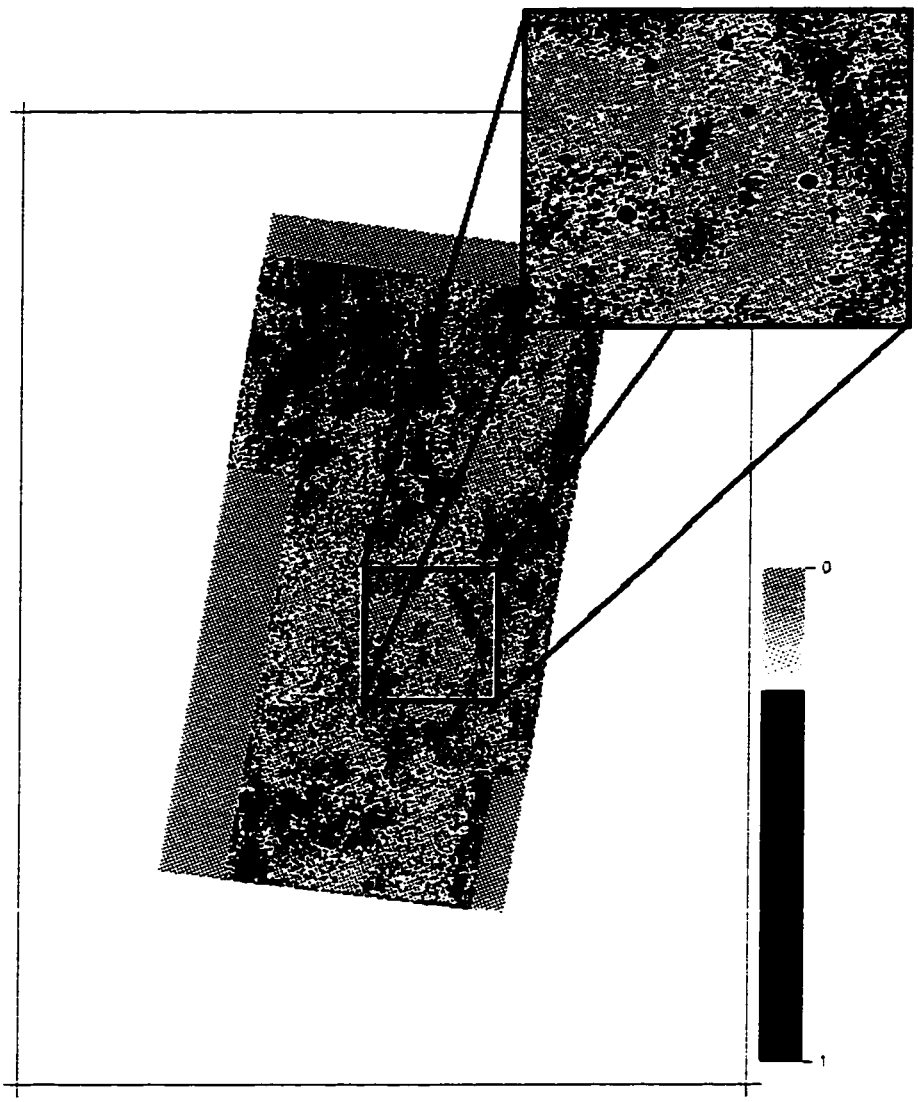

Figure 26: Volume of silt map generated showing the multi-attribute driven volume of silt. To generate this map19 wells out of 21 wells were used (well A and well I were neglected). Note that this method recognizes the difference between well A and well I without including them in the analysis. The variations between well A and well I can be seen in the zoomed version (upper right corner).

CHAPTER 5

Results

This study provides two types of results, quantitative and qualitative. The quantitative result is the one which gives values of reservoir properties over the whole seismic survey within seismic lateral resolution. The qualitative result is the one at which each attribute is related it to a physical explanation and on the bases of all the attributes, a consistent interpretation is drawn. The quantitative result and the qualitative one should converge and lead to the same conclusion.

Quantitative Results

In this research, porosity, water saturation, and volume of silt maps are the results of the multi-seismic-attributes driven reservoir properties method used (Figs. 5, 25, 26).

From the porosity map (Fig. 5), the area is very complicated and the porosity varies dramatically from place to place which makes it very difficult to predict porosities using only well information because of the sparsity of control points. The reason for the complexity is that the high porosity areas are located in the filled wadis, eolian sand deposits and channel deposits (see Geology of the Area Section). The lithology is not homogeneous, so porosity is not either. The blue to violet colors

show low porosities, less than 0.09, and the yellow shows the high porosities, greater than 0.09.There is a NNE-SSW trend of high porosities.

The crossplot of the original porosity values versus calculated ones (Fig. 27) shows that the obtained porosities have a fair correlation with the original ones. Well A and well I are marked by their letters. Neither of these wells were used in obtaining the relationship between seismic attributes and reservoir properties. The crossplot shows that there is a large error in estimating the porosities of the neglected wells, but it also shows that well I has a higher porosity than well A. These differences cannot be detected if the well information are only used in producing the porosity map. Hence, seismic data can be of a great help in detecting the lateral small changes in reservoir properties.

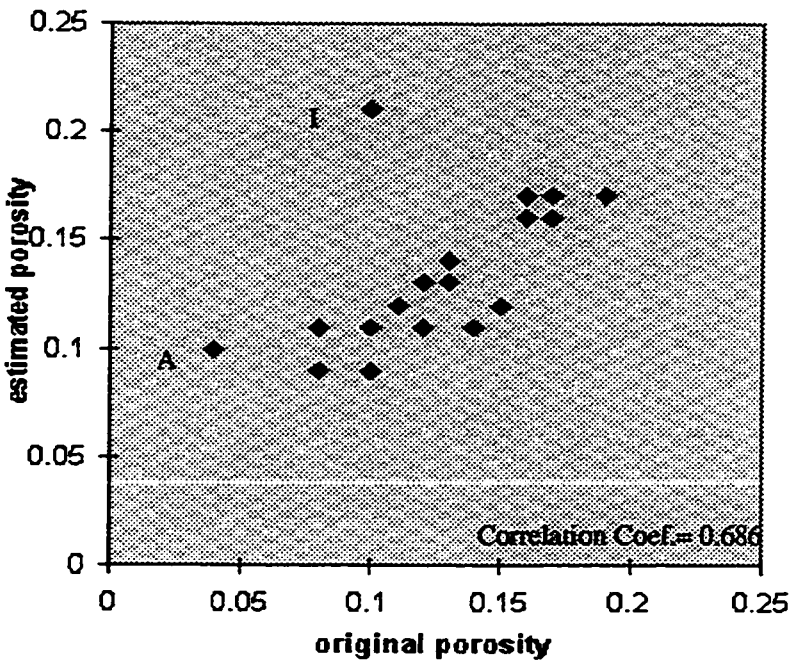

Figure 27: Original porosity versus calculated porosity.

To generate the above crossplot, values from well logs were used in addition to the values calculated using seismic attributes which were extracted from the trace near-

est to a well. If we look at the values of the reservoir properties on the reservoir property maps we will find the seismic-driven reservoir properties very good both in relative and absolute sense, because at the large scale so our eyes filter out the random noise. However, in the crossplot we are looking at a single trace nearest to a well, which makes the noise strongly affect the results.

The water saturation map also shows the reservoir complexity (Fig. 25). The high porosity zone has a relatively low water saturation, less than 0.7, surrounded by higher water saturation values. The area of low water saturation is structurally high, so hydrocarbon migrated towards it. Crossplot of the original water saturations versus calculated ones shows a relationship with correlation coefficient of 0.5 (Fig. 28). There are errors in predicting the exact values of wells A and I, but the relative values are reasonable.

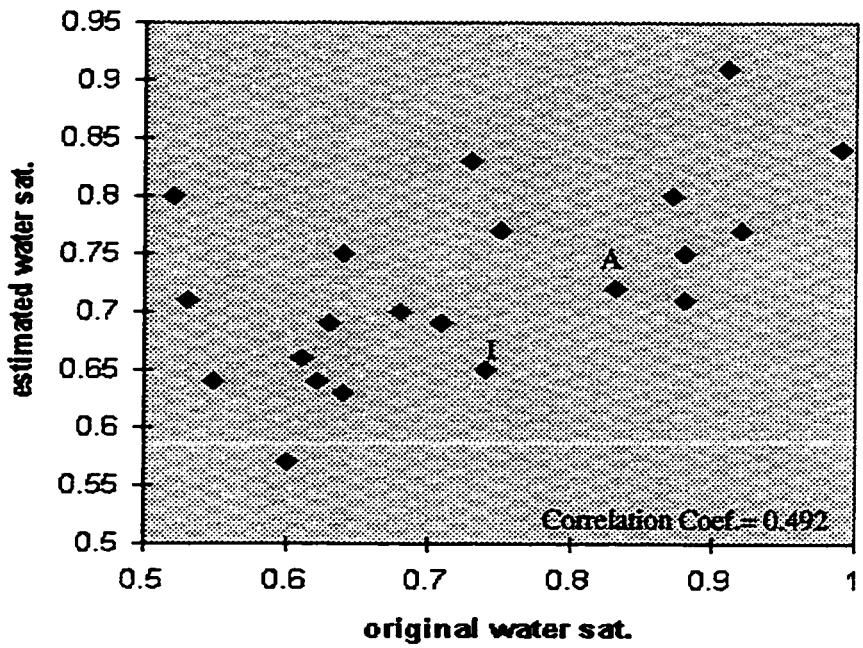

Figure 28: Original water saturation versus calculated one. Fair correlation coefficient.

The volume-of-silt map (Fig. 26) shows a less amount of silt at areas of high porosities and low water saturation. Crossplot between original values of the volume-of-silt versus calculated ones shows that there is a linear relationship between them with a correlation coefficient of 0.54 (Fig. 29).

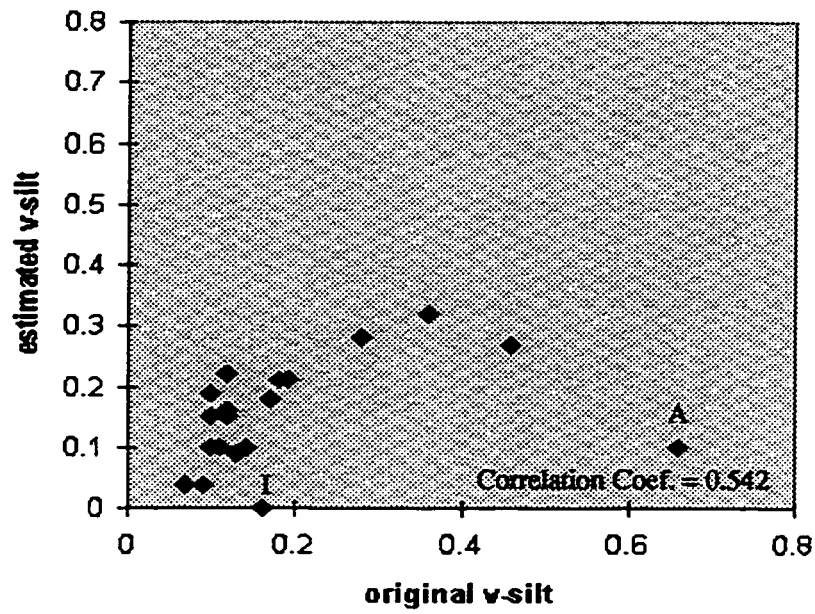

Figure 29: Original volume of silt versus calculated one. Good correlation coefficient.

By combining the results of the three reservoir property maps, we can indicate good areas to be targeted in the future drilling programs.This map is produced using the following equation:

Indicator map = (POR-0.1)+(0.6-WSAT)+(0.3-VSILT)

The terms of this equation were chosen such that porosity values greater than 0.1 are considered to be good porosities. Similarly, water saturations are considered to be good when they are less than 0.6; and good values for volume-of-silt are below 0.3. The indicator map shows that there is a trend going from the center of the survey to NE corner with positive values which means promising locations (Fig. 30). Overall, the seismic-multi-attributes driven reservoir properties method proved to show results with lower errors than using geostatistics of well information only.

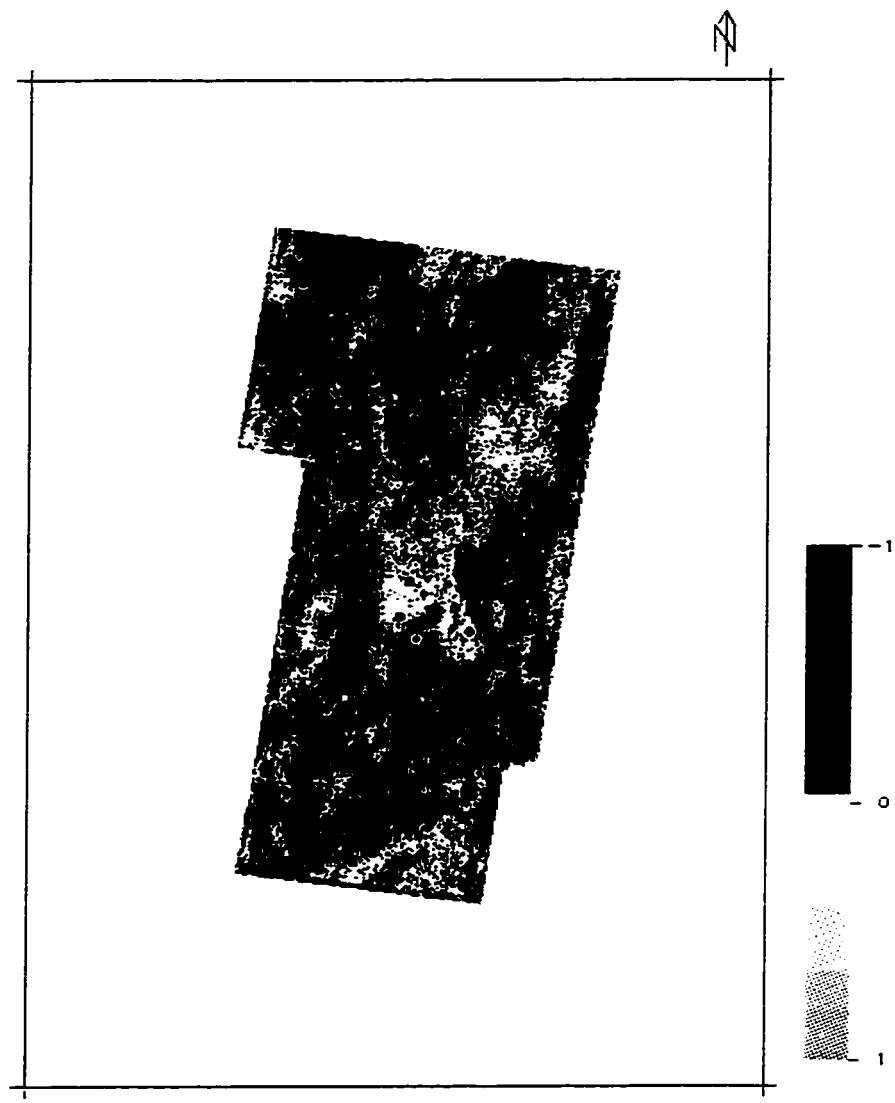

Figure 30: A map indicating the reservoir quality using the following equation: Value = (por-0.1)+(0.6-wsat)+(0.3-vsilt). Yellow to brown colors are considered to reflect good reservoir quality. The higher the positive number, the better the reservoir.

Error Correction

A linear relationship was used to predict reservoir properties from seismic attributes.This relationship cannot honor all of the well information. As a result, errors are expected in the predicted reservoir properties (Fig. 32).

To correct for these errors, an error map was generated using simple kriging of the errors calculated at well locations. These errors are the differences between the original reservoir properties calculated from logs and the predicted ones. After that, the error map was added to the predicted porosity map (Figs. 31 - 34). The resultant map shows similar trends to the original predicted map with the conclusion that good reservoir properties are available at the center and going toward the NE corner of the survey, and low quality reservoir properties would be at the southern part.

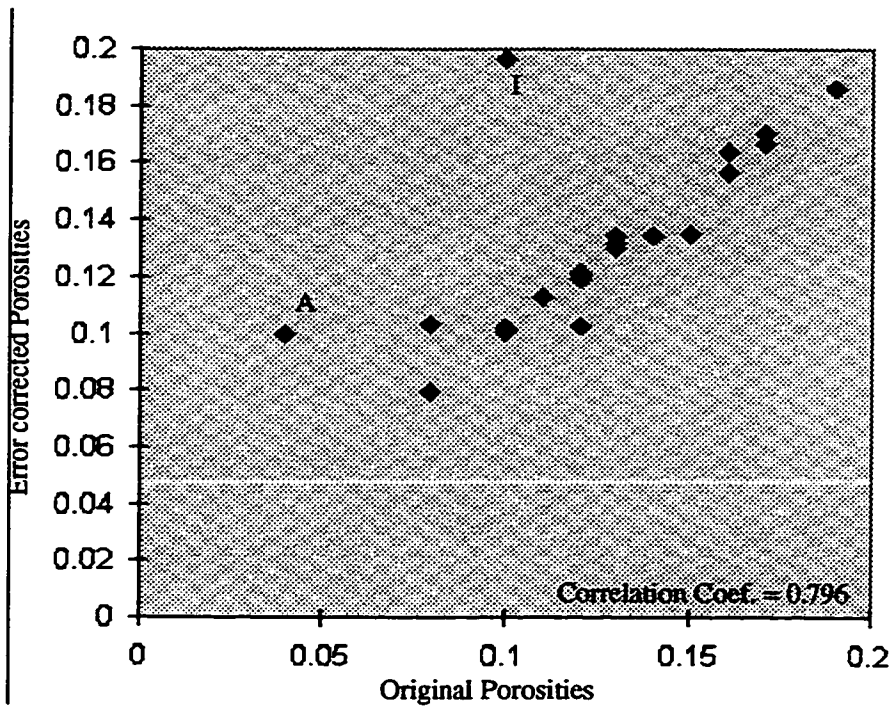

Figure 31: Cross plot of original porosities versus corrected porosities. The pink dots represent wells A and I. Note the improvement of the correlation coefficient.

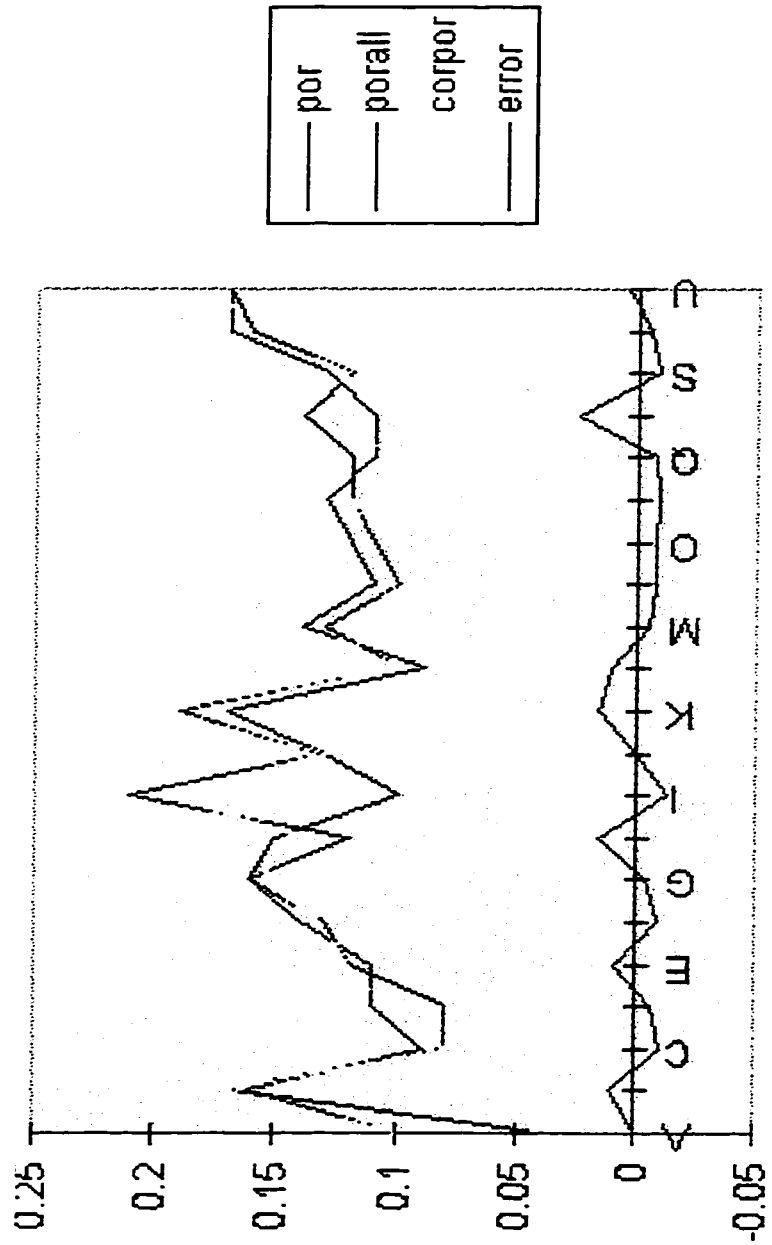

Figure 32: Original porosities (black), calculated porosities (pink), error corrected porosities (yellow), and the error curve (blue).

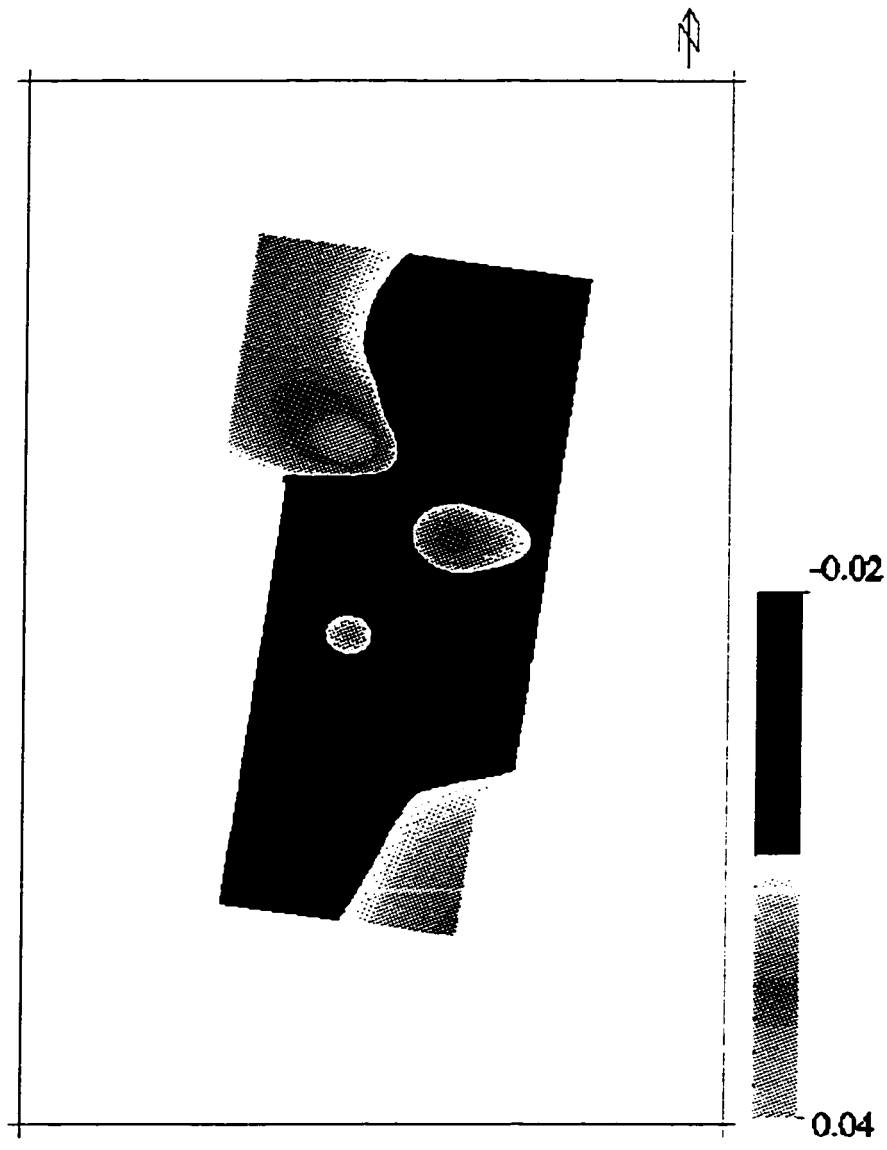

Figure 33: The error map generated by kriging the errors at well locations.

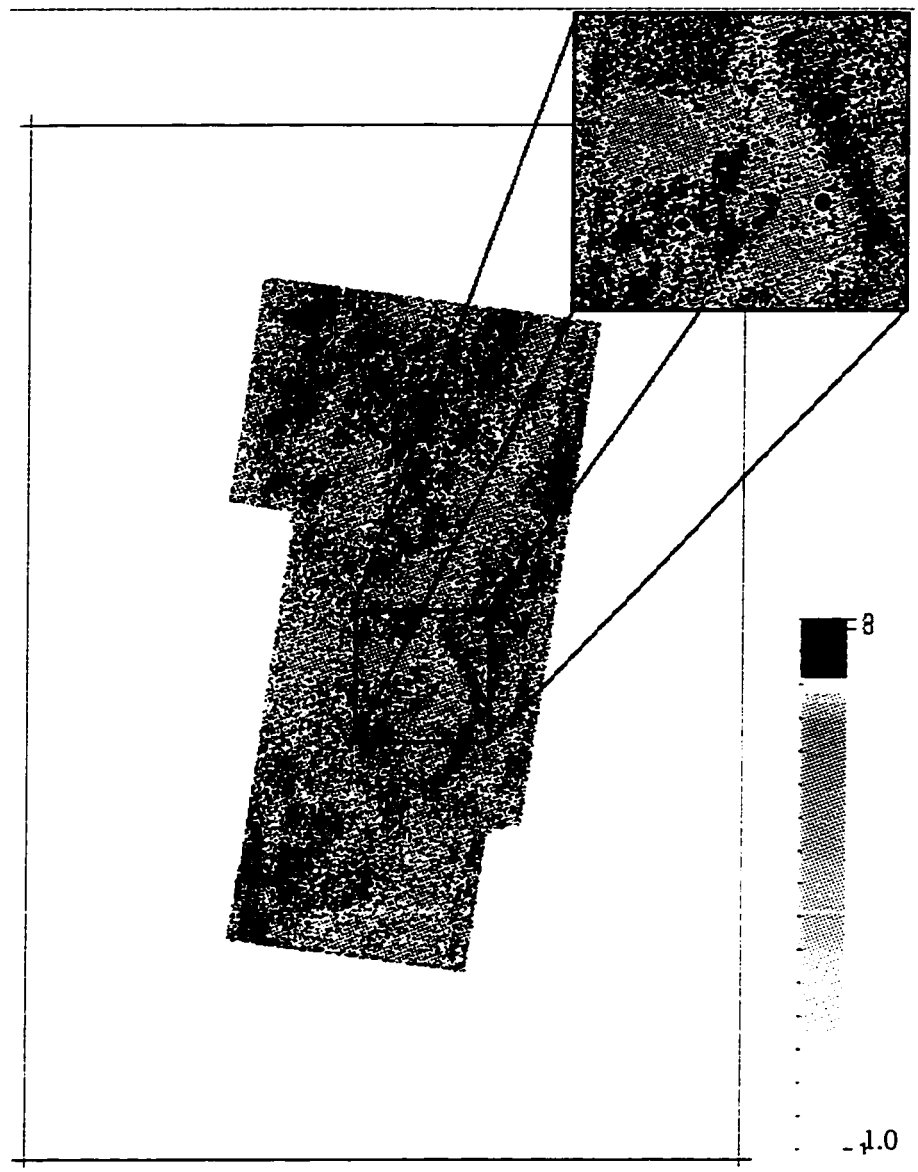

Figure 34: The error-corrected porosity. The error map was added to the predicted porosity map.The variations between well A and well I can be seen in the zoomed version (upper right corner).

Qualitative Results

In this section, some of the seismic attributes are going to be used to interpret the area of interest qualitatively. These attributes are the amplitude statistics, peak spectral frequency, and spectral slope from peak to maximum frequency, and dominant frequency series, f1, f2, and f3 (Figs. 35, 36, 37, 38, 39).

Amplitude statistics are showing almost similar trends. Only the average absolute amplitude map (Fig. 14) will be interpreted. This attribute map shows that there are very high amplitudes, violet to blue, at the northern part of the survey. These high amplitudes started almost at the center of the survey and extended toward the north eastern corner. The high amplitudes may show lithology changes. In this situation, this attribute can be used as a good indicator of the quality of the zone of interest. The higher the amplitude, the higher the porosity and the higher the hydrocarbon saturation. However, high amplitudes may also be caused by tuning phenomena. In the study area used in the research, the high amplitudes are actually caused by both lithology and tuning phenomena (see the section on tuning).

Peak spectral frequency, and dominant frequency series are showing similar trends. Peak spectral frequency will be used for the interpretation (Figs. 35, 37, 38, 39). This attribute shows that there are relatively low frequencies at the southern part of the survey and at the north eastern corner. A porous zone with hydrocarbons filling the pores absorbs the high frequencies faster than a solid rock. As a result, the lower the frequency, the better the reservoir. Comparing the peak spectral frequency map and the average absolute amplitude map, it is evident that almost from the center of the survey going toward the north east corner, high amplitudes and low frequencies are encountered which is promising. However, at the southern part, the amplitudes are not high but the frequencies are still low. If the zone at the southern part is a porous zone then high amplitudes should be available which is not the case. The frequencies may be attenuated somewhere above the zone of interest in the southern part.

The map of the spectral slopes from peak to maximum frequencies shows that there are large negative slopes at the area from the center of the survey to the north eastern corner and low slopes at the southern part of the survey (Fig. 36). The two black lines surround the low spectral slopes which may be related to the silt body available in this area (see the geology section). High negative slopes indicate fast absorption of high frequencies which is a property of porous zones filled with hydrocarbon.

Combining average absolute amplitude, peak spectral frequency, and spectral slopes from peak to maximum frequencies, indicates that the area from almost the center of the survey going to the north is a promising one while the rest is not.

The porosity map shows a similar trend with relatively high porosities. Water saturation is showing a reasonable water saturation occurring along the same trend. Moreover, the volumes-of-silt map shows low values at the same places. At the southern part, surrounded by the two black lines, the volume of silt is relatively high which was identified by the spectral slope attribute.

Agreement between different attributes and between qualitative and quantitative interpretation increases the confidence in the ability of this method to predict reservoir properties.

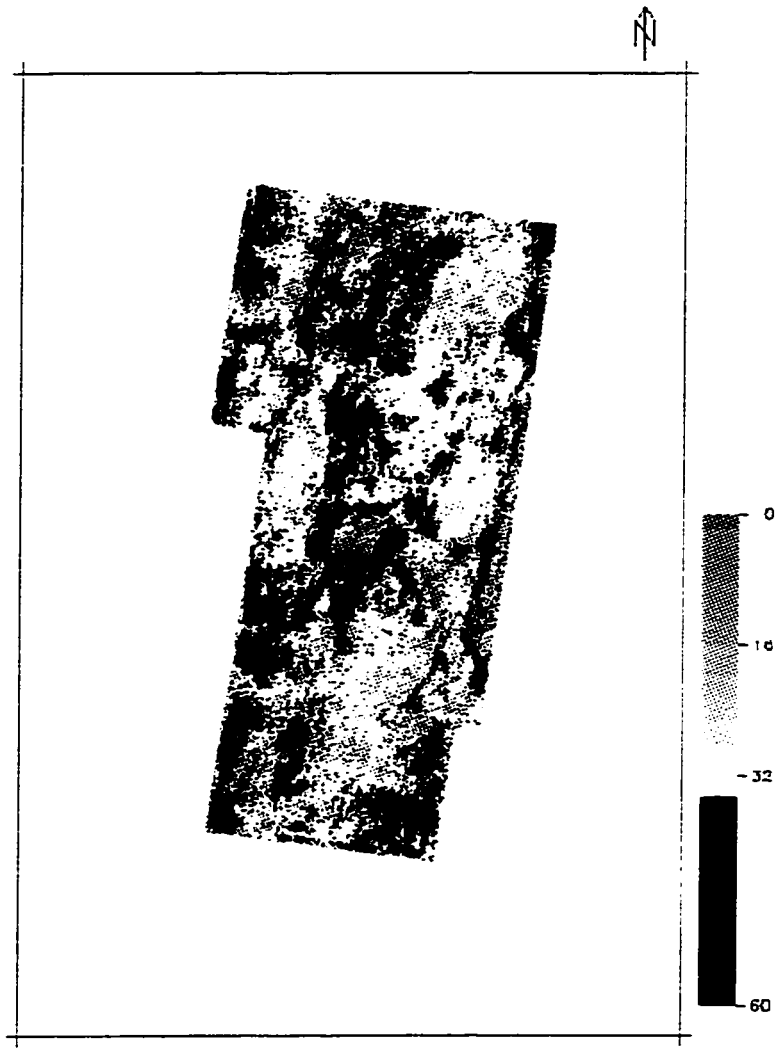

Figure 35: Peak spectral frequency. Low frequencies indicate a porous zone with hydrocarbons filling the pores.

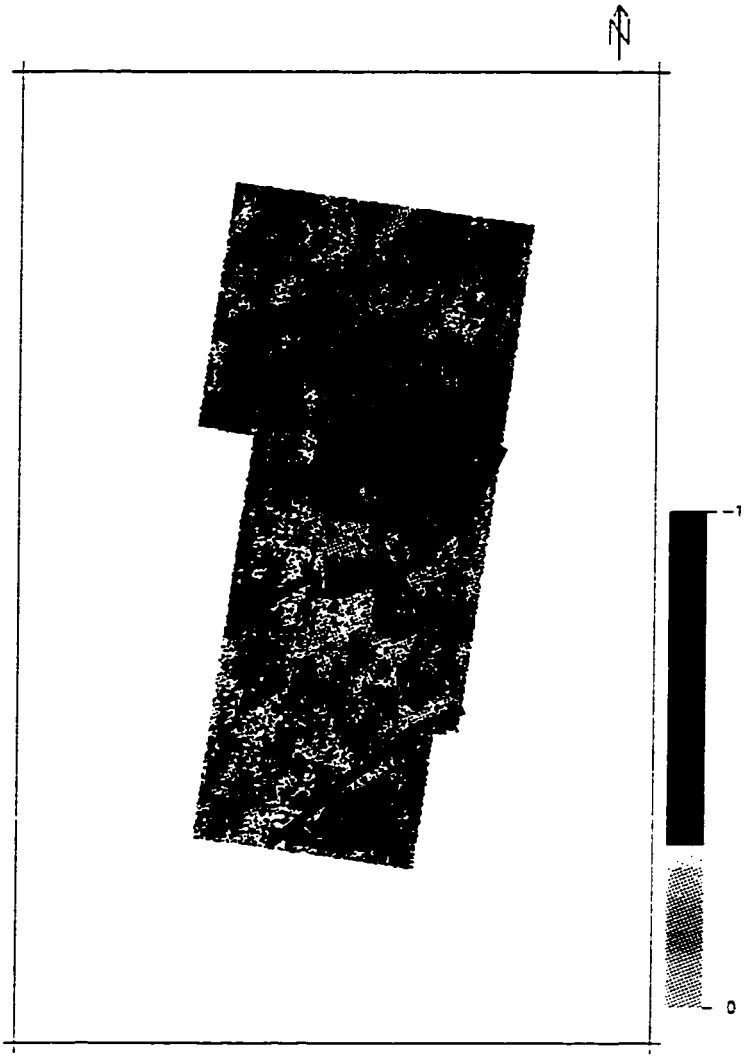

Figure 36: Spectral slope from peak to maximum frequency. The area surrounded by the two black lines is the silt body which is showing low slopes.

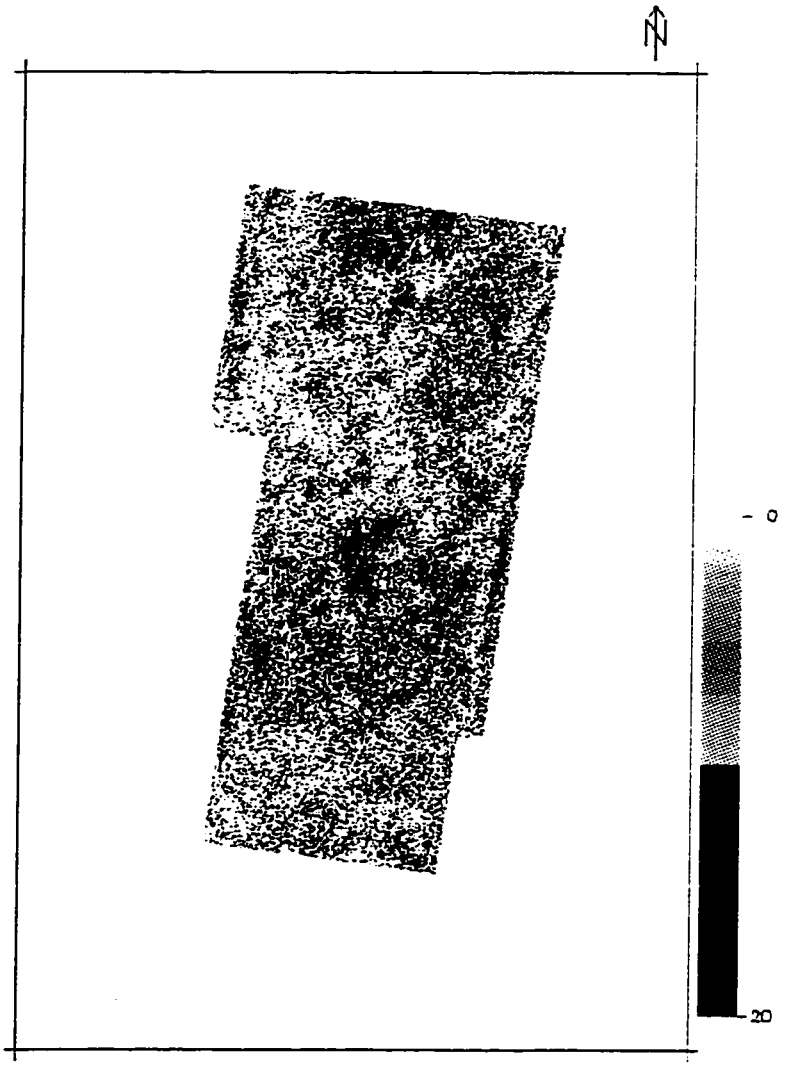

Figure 37: F1 dominant frequency.

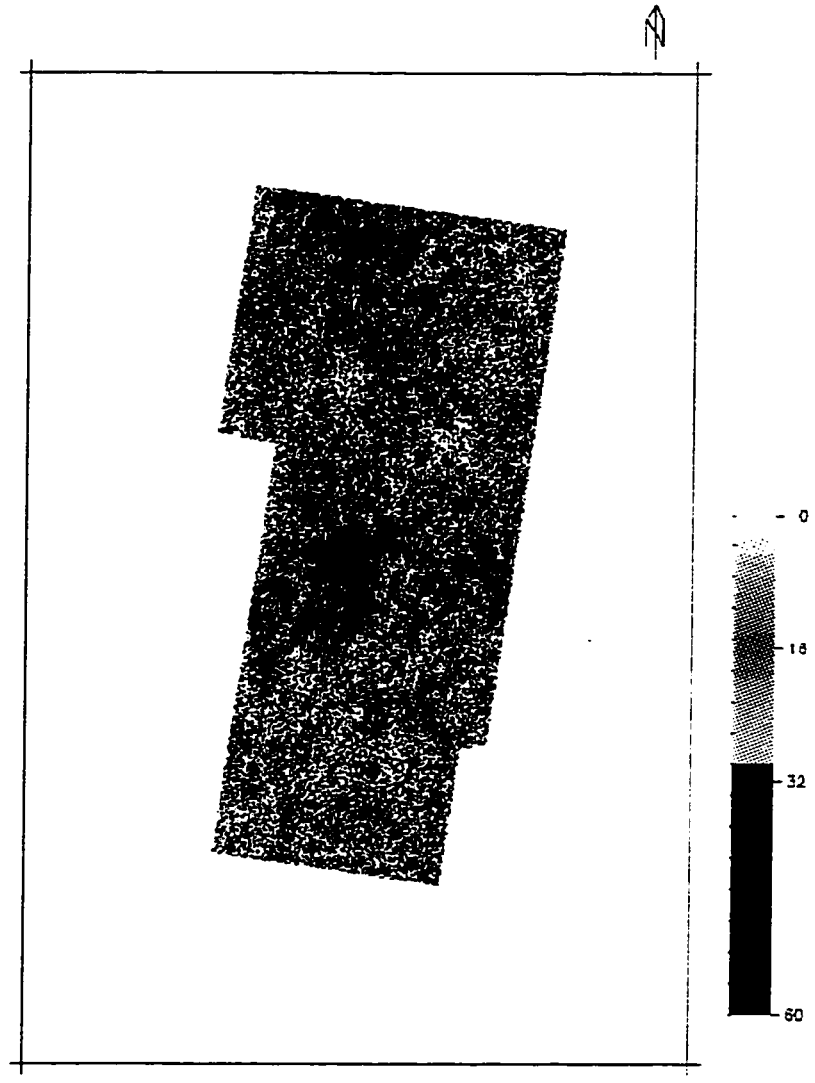

Figure 38: F2 dominant frequency.

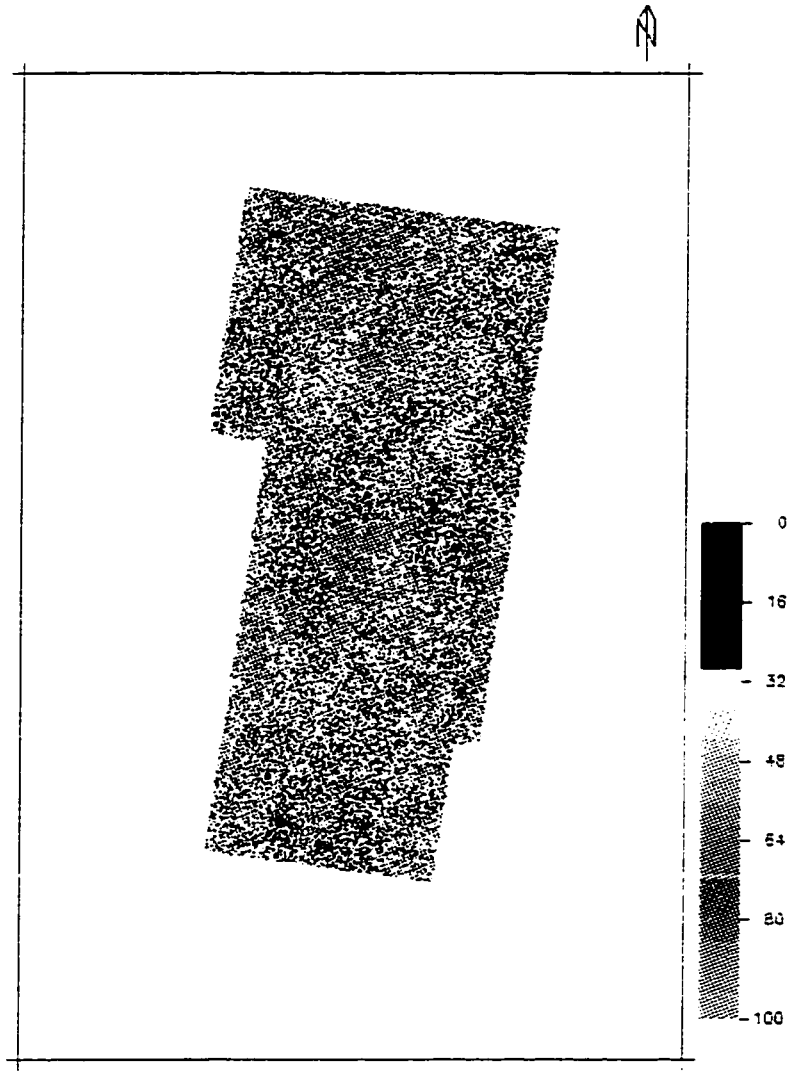

Figure 39: F3 dominant frequency.

Tuning Phenomena

Amplitude increase or decrease does not always reflect lithology. Sometimes, it is related to the geometry of the layers. Tuning phenomena are very important to be understood in order to be fully taken into account in the interpretation.

If the bed thickness is greater than the wavelength, there is no interference between wavelets coming from the upper and lower interfaces of the targeted zone. Wavelet interference starts as soon as bed thickness becomes smaller than the wavelength. This interference can be constructive or destructive depending on the polarity of the two wavelets coming from the top and the bottom interfaces of the layer of interest. For wavelets of opposite polarity, the interference will be constructive, and for wavelets with the same polarity the interference will be destructive (Robertson, 1984). Amplitude tuning, which is the occurrence of maximum amplitude, occurs when the bed thickness in two way time becomes half the period (see wedge model section). On the interval from tuning to zero thickness, the seismic method does not provide any thickness information. Thickness information can be only inferred from the amplitude variations (Widess, 1973).

Wedge Model

A wedge model was generated to study the effect of tuning on different seismic attributes. This model consists of a sand layer with velocity of 11000 ft./sec. pinching out against a shale layer with velocity of 13000 ft./sec. Below the sand layer, there is another shale layer with velocity of 13000 ft./sec. (Fig. 40).

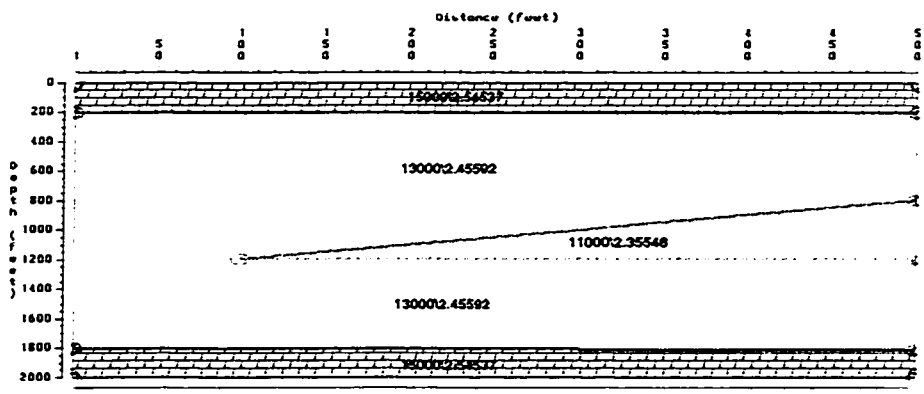

Figure 40: Wedge model to study the tuning effect.

The lower sand-shale interface is horizontal while the upper one is dipping with 4.8 ft./trace. The two interfaces join at trace number 19. Vertical ray tracing was applied to simulate a migrated seismic section. The resultant reflection coefficients were convolved by a 25 HZ Ricker wavelet (Fig. 41). The predominant period of this wavelet is theoretically 40 msec. However, when measured manually, it appears to be only 33 msec. instead of 40 msec. Hence the 33 msec. period will be used in the calculations.

The interference started when the thickness became 33 msec. which is the period of the wavelet (or 181.5 ft. which is the wavelength). At that point, the amplitude started increasing until it reached its maximum, about 1.4 times the amplitude in the thick zone, when the thickness becomes half the period. When the true thickness is less than the period of the wavelet, the apparent thickness will be lower than the true thickness until the true thickness becomes almost half the period of the wavelet, then both the true and the apparent thicknesses will be the same. As the thickness becomes lower than half the period, the amplitude decreases until it reaches zero and the apparent thickness stays almost constant. In the interval from half the period thickness until zero thickness, there is no thickness information in the seismic data (Fig. 42). However, thickness can be approximated using the following equation:

$$Thickness = \frac{A\lambda_b}{4\pi A_{thick}}.$$

where A is the tuned amplitude, λ_b is the predominant wavelength, and A_{thick} is the amplitude when the bed is thick (Widess, 1973).

a)

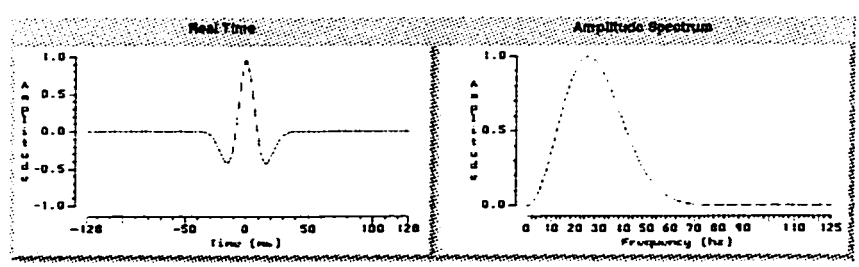

b)

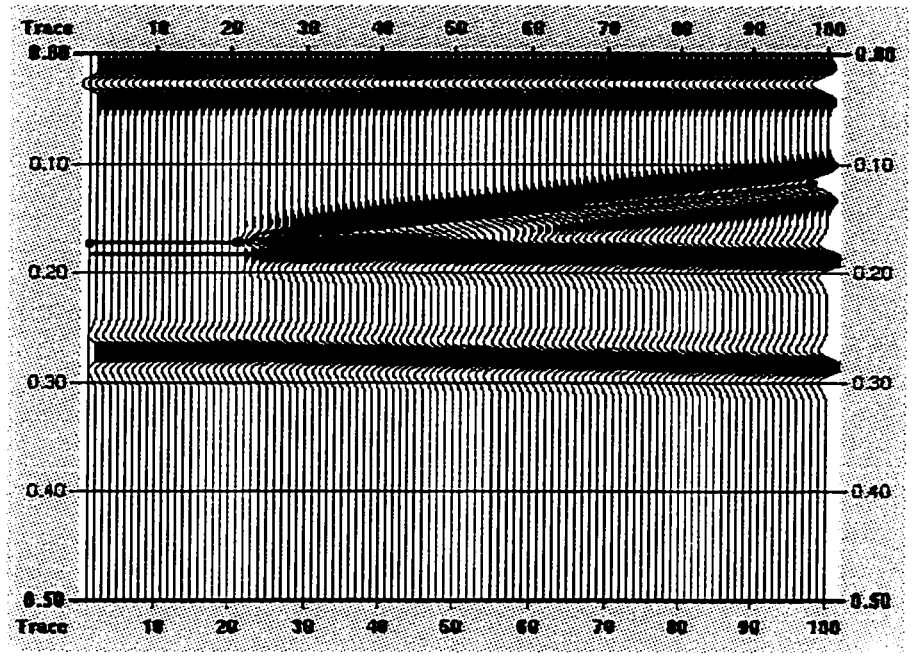

Figure 41: The Ricker wavelet (a) and the synthetic traces (b) generated using the wedge model.

Different seismic attributes of the wedge synthetic traces were calculated to see if they could provide a better definition of the thin layer. The attributes were extracted on the lower interface of the wedge and plotted against CDP number (Fig. 43). Most of the attributes are showing anomalous values at the location of pinching out around cdp 19. This location is very difficult to detect using conventional seismic displays.

When we look at the absolute amplitude map (Fig. 14), we see high amplitudes occurring at different locations.The question is what is the cause of these high amplitudes. Do these high amplitudes reflect the lithology or the geometry of the beds? In order to answer these questions, we need to look at the isochron versus average absolute amplitude crossplot (Fig. 44). This figure shows that there are high amplitudes when the thickness is around 23 msec. These high amplitudes are most probably caused by tuning. After the tuning thickness, the maximum amplitudes become constant as the thickness increases.

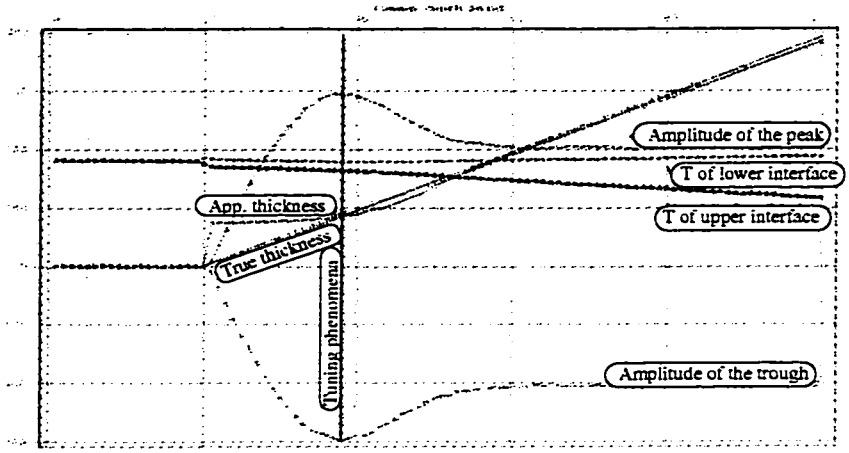

Figure 42: Amplitude, apparent thickness, true thickness and time of lower and upper wedge interfaces versus cdp.

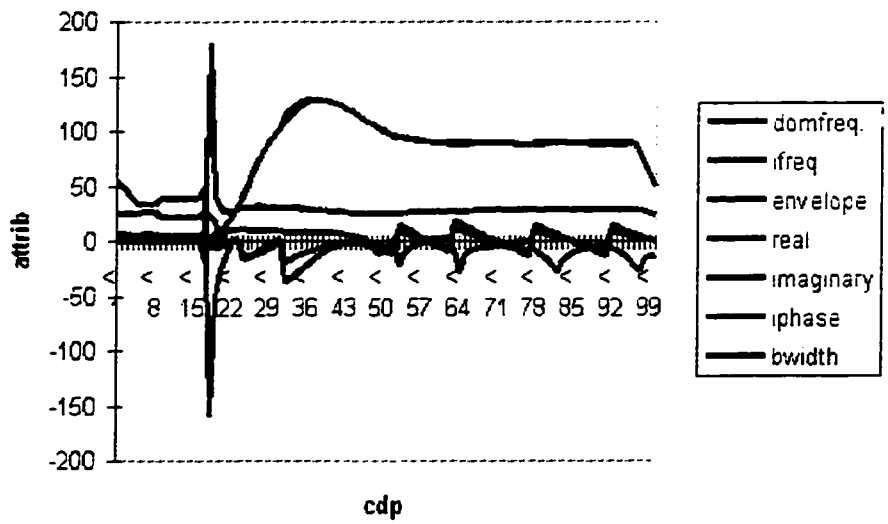

Figure 43: Different attributes of the wedge model. Most of the attributes have anomalous values where the bed is pinching out

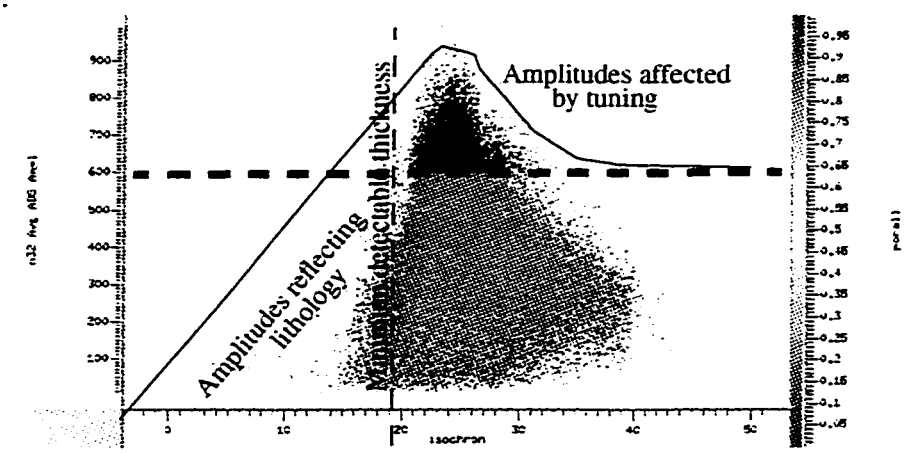

Figure 44: Isochron versus average absolute amplitude with an envelope drawn using black line. The black dots are the amplitude anomalies probably caused by tuning.

By drawing a horizontal line connecting the highest amplitude at the thick part and extending this line to the thin part, we can separate the amplitude increases caused by tuning from those caused by lithology. The area which contains the tuned amplitude is selected and displayed on the map of isochron (Fig. 45).

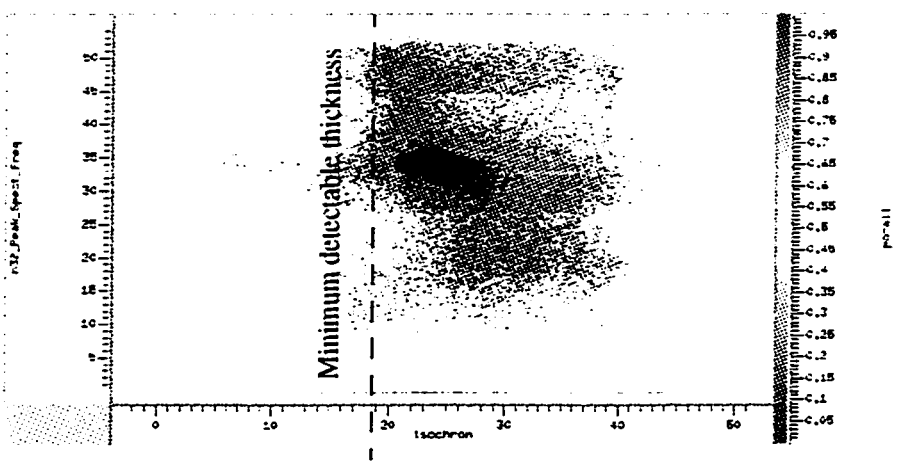

Figure 46: Peak spectral frequency versus isochron. The black points represent the amplitude anomalies caused by tuning.

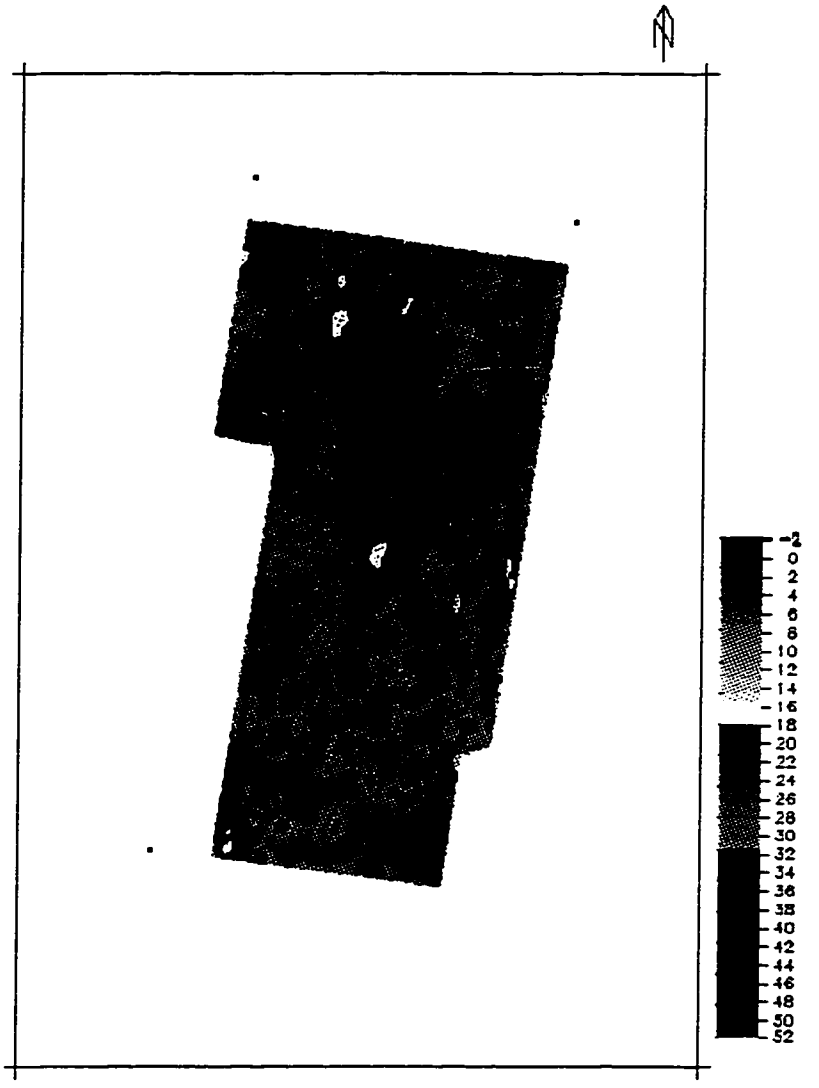

Figure 45: Isochron map overlain by areas at which amplitudes are affected by tuning (red points).

The selected samples are highlighted on the average absolute amplitude versus isochron crossplot (Fig. 44) and on the peak spectral frequency versus isochron crossplot (Fig. 46).

Seismic response does not reflect only lithology, it also reflects noise. Noise should be considered when interpreting seismic data. The tuning phenomenon is a type of noise which cannot be removed from the data. Tuning affects both the amplitude and the thickness of the layer of interest (Figs. 44, 46). Both of these figures show that the minimum thickness is around 18 msec., which is half of the period if we consider the frequency in the data to be 25 Hz. From the wedge model, we saw that the apparent thickness stays almost constant when the true thickness is half the period of the wavelet in the seismic data or lower.

CHAPTER 6

Validation

The original predicted maps were used to validate the use of multi-seismic-attribute method in predicting reservoir properties, not the error corrected ones. To test the validity of this method, two of the wells, well A and well I were preserve from the beginning and not used in any step of the attribute analysis performed. Then the reservoir properties at these two wells were compared with the predicted values.

Kriging Versus Attributes Driven Reservoir Properties

Simple kriging of reservoir properties using only well information shows that this method cannot predict the correct values at the neglected wells, wells A and I (Figs. 3, 4). The porosity map generated by kriging the information from only 19 wells out of 21 could not predict the variations between well A and well I. Well A has a porosity of 0.04 while well I has a porosity of 0.10. This variation can be seen in the other porosity map generated by kriging all the 21 wells (Fig. 4).

The multi-seismic-attributes driven porosity map shows variations between the locations of well A and well I, though these two wells were not used in calculating the porosity map (Figs. 5, 47). Consequently, seismic data should be used in predicting variations between wells.

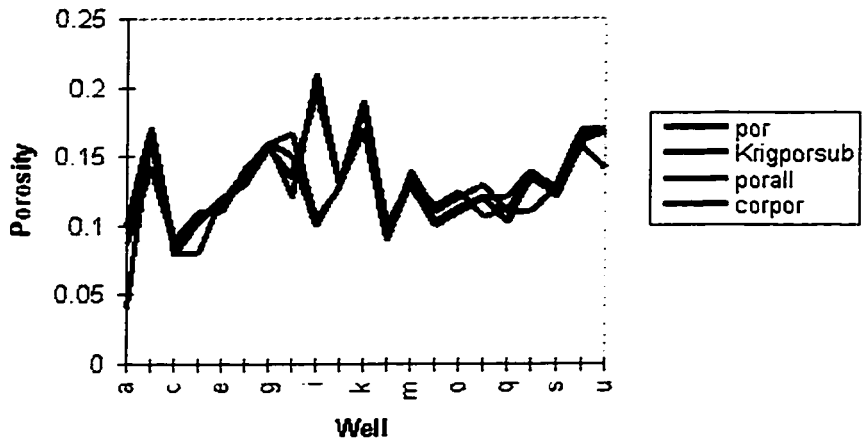

Figure 47: Comparison between original porosity(por), kriged porosity(krigporsub), seismic attributes estimated porosities(porall), and error corrected seismic attributes estimated porosities(corpor).

Original porosities versus predicted ones, original volume of silt values versus predicted ones, and original water saturation values versus predicted ones of the two neglected wells, well A and well I, show errors in predicting exact reservoir properties. However, the relative predicted values are very reasonable (Figs. 27, 28, 29).

Single-Attribute Versus Multi-Attributes

The single-attribute-driven reservoir properties method is another way of using seismic attributes for quantitative reservoir interpretation. This method selects the seismic attribute showing the maximum correlation with a specific reservoir property, obtains a relationship to approximate the reservoir properties, and finally applies this relationship to the whole volume of seismic data.

The main difference between the single attribute method and the multi-attribute method, as indicated by the name, is the number of attributes analyzed. In this research, it is found that the multi-attribute analysis is more accurate in deriving the

reservoir properties than the single attribute method. Seismic attributes show the seismic data from different angles, each attribute revealing different characteristic of the seismic data. When combining all these seismic characteristics we may get a better description of the reservoir than using only a single attribute. For example, variations in the amplitude attribute cannot be related only to lithology, as they are also affected by tuning phenomena. The instantaneous frequency attribute can help in deciding wether the amplitude variations found in any of the amplitude attributes are due to tuning or any other effect. Consequently, using both of the above attributes provides the interpreter with a better explanation of the reservoir. Moreover, according to this research, as the number of the attributes used in the calculation increases the results get better.

Figure 48 shows the sum of squared residuals, which is the sum of the squared differences between the original reservoir property values and the predicted ones for all wells, when using only one seismic attribute to predict the reservoir property.

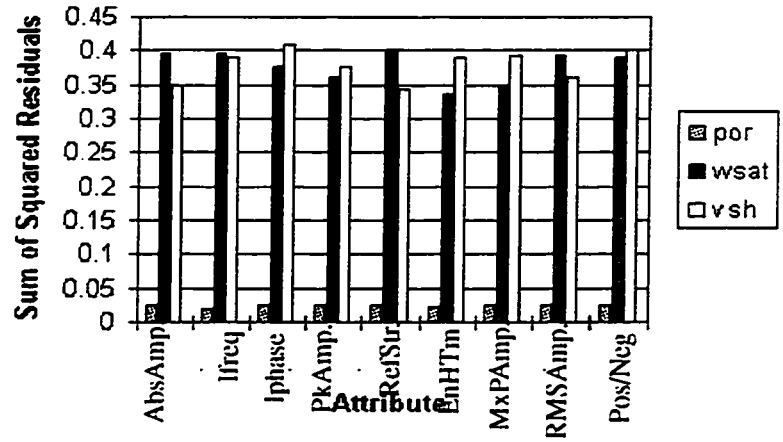

Figure 48: The sum of squared residuals for using a single attribute to predict reservoir properties, porosity, water saturation and volume of silt.

Instantaneous frequency showed the lowest error of 0.02 when it is used to predict the porosities. Energy half-time shows the lowest error of 0.34 when it is used to

predict water saturation. And, reflection strength shows the lowest error of 0.34 when calculating volume of silt values.

Figure 49 shows the number of attributes used in the reservoir properties prediction process versus the sum of squared residuals of porosity, water saturation and volume of silt. The figure started with one attribute in the left hand side and ended with nine attributes which have been used in the process of predicting the reservoir properties in this research.

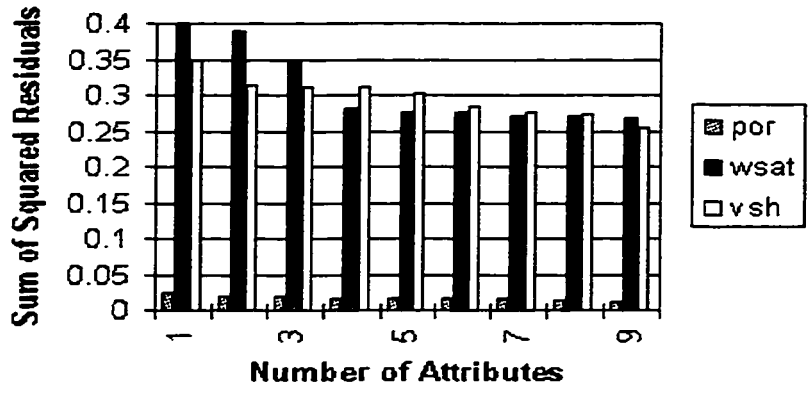

Figure 49: Number of attributes used in the analysis versus the sum of squared residuals. As the number of attributes increases the error decreases.

The first attribute used in Fig. 49 is the average absolute amplitude alone; the instantaneous frequency attribute was then added; then average peak amplitude; then average reflection strength; then energy half-time; then maximum peak amplitude; then RMS amplitude; and finally the positive-to-negative ratio attribute was added to get a total of nine attributes used in the analysis. This process was performed three times to see the effect of increasing the number of attributes in calculating different reservoir properties, one for porosity, one for water saturation, and another one for volume of silt. The figure shows that as the number of attributes increases, the error decreases. It seems that, after a specific stage, a farther increase in the number of seismic attributes does not improve the solution any more.

Comparing the errors resulting from using only one attribute (the absolute amplitude) with those from using nine attributes, we found that the error of the single-attribute prediction method is 2.40 times the error of the multi-attribute prediction method when predicting porosity, 1.48 times that when predicting water saturation, and 1.37 times that when predicting the volume of silt. Moreover, if we compare the errors in calculating the reservoir properties using the single attribute that shows maximum correlation with the reservoir properties, and the errors found using nine attributes, we found a 1.96 times improvement when calculating porosity, 1.25 times improvement when calculating water saturation and 1.36 times improvement when calculating volume of silt.

The best correlation coefficients between reservoir properties and single attributes were 0.4415 between porosity and instantaneous frequency, 0.3983 between water saturation and energy half-time, and -0.4065 between volume of silt and reflection strength.The correlation coefficient between the single-attribute- driven reservoir properties and the original reservoir properties will be the same as the correlation coefficient between the seismic attributes used in the analysis and the original reservoir properties. For example, if we use the seismic attributes showing the best correlation with the reservoir properties in the single attribute analysis, the resultant correlation coefficient between the predicted reservoir properties and original ones will be 0.4415, 0.3983, and -0.4065 for porosity, water saturation, and volume of silt, respectively. However, if we calculate the correlation coefficient between the multi-seismic-attributes driven reservoir properties and the original ones, we will get 0.686 for porosity, 0.492 for water saturation, and 0.542 for volume of shale. By comparing the correlation coefficients between predicted reservoir properties and original ones using the single-or the multi-attributes driven reservoir property methods, it is evident that the correlation coefficient increases when using multi-attributes approach.

From the above discussion we can conclude that using multi-seismic-attributes approach in deriving the reservoir properties is better than using only a single-seismic-attribute. However, each attribute should have new information and it should not be a linear transformation of other attributes used in the analysis.

Conclusion

Integrating data from different fields is very important in getting a better description of a reservoir. Well information has a very low spatial resolution and a high vertical resolution, while seismic data has a high spatial resolution and a low vertical resolution. As a result, to get a better description of a reservoir, all available data such as geophysical, geological and petrophysical data need to be integrated.

The multi-seismic-attributes driven reservoir properties method proved to be useful in utilizing seismic data and well information to predict reservoir properties. This research proved that this method is better than predicting reservoir properties using kriging of well information or using the single seismic attribute approach to estimate reservoir properties.

In this research, seismic attributes were interpreted quantitatively and qualitatively. In the quantitative part, nine attributes were analyzed to predict values of porosity, water saturation, and volume of silt over the whole seismic survey. In the qualitative part, five spectral attributes were added to the previous nine attributes used in the quantitative part. The fourteen attributes were studied qualitatively trying to get a consistent interpretation. Convergence of qualitative and quantitative interpretations increases the confidence in the attribute analysis methodology used in this research.

References and General Bibliography

Al-Laboun A., "Unayzah Formation: A New Permian Carboniferous Unit in Saudi Arabia", AAPG, Vol.71, No.1, Jan. 1987, P. 29-38.

Brown A.R., R. Wright, K. Burkart, W. Abriel, and R. McBeath, "Tuning Effects, Lithologic Effects, and Depositional Effects in the Seismic Response of Gas Reservoirs", Presented at the 46th Annual Meeting of EAEG, London, England, June 21, 1984.

Chen Q. and S. Sidney, "Seismic Attributes Technology for Reservoir Forecasting and Monitoring", The Leading Edge, Vol.16, No.5, May 1997, P.445-456.

Enachesw M. E., "Amplitude Interpretation of 3-D Reflection Data", The Leading Edge, Vol.12, No.6, June 1993, P.678-685.

Gastaldi C., "Reservoir Characterization from Seismic Attributes: An Example from the Peciko Field (Indonesia), The Leading Edge, Vol.16, No.3, March 1997, P.263-266.

Hardage B.A., D.L. Carr, D.E. Lancaster, J.L. Simmons, D.S. Hamilton, R.Y. Elphick, K.L. Oliver, and R.A. Johns, "3-D Seismic Imaging and Seismic Attribute Analysis of Genetic Sequences Deposited in Low-Accommodation Conditions", Geophysics, Vol. 61, No.5, Sep-Oct 1996, P.1352-1362.

Hirsche K. and J. Porter, "The Use and Abuse of Geostatistics", The Leading Edge, Vol.16, No.3, March 1997, P.253-260.

Kalkomey Cynthia T., "Potential Risks when Using Seismic Attributes as Predictors of Reservoir Properties.", The Leading Edge, Vol.16, No.3, March 1997, P.247-251.

King A.W., "Semi-Arid Distal Alluvial Fan Deposits of the Permian Unayzah Formation Along the Nuayyim Trend, Central Saudi Arabia", GeoArabia, Vol. 1, No. 1, March 1996, P. 158.

Landmark, "PostStack/ Pal user Guide", Landmark Graphics Corporation, Houston, Texas, Oct.1996, P. 1-412.

Lewis C., "Seismic Attributes For Reservoir Monitoring: A Feasibility Study Using Forward Modeling", The Leading Edge, Vol.16, No.5, May 1997, P.459-469.

McGillivray J.G., and M.I. Husseini, "The Paleozoic Petroleum Geology of Central Arabia", AAPG, Vol.76, No.10, Oct. 1992, P. 1473-1490.

Neidell N.S., and E. Poggiagliolmi "Stratigraphic Modeling and Interpretation-Geophysical Principles and Techniques", AAPG, Memoir 26, 1997, P.231-250.

Pennington W.D., "Seismic Petrophysics: An Applied Science for Reservoir Geophysics", The Leading Edge, Vol. 16, No.3, March 1997, P.247-251.

Robertson J.D. and H.H. Nogami, "Complex Seismic Trace Analysis of Thin Beds", Geophysics, Vol.49, No.4, Apr.1984, P.344-352.

Sheriff R.E., "Limitations on Resolution of Seismic Reflections and Geologic Details Derivable from Them", AAPG, Memoir 26, 1997, P.3-14.

Schultz P., S. Ronen, M. Hattori, and C. Corbett, "Seismic-Guided Estimation of Log Properties, Part 1", The Leading Edge, May 1994, Vol.13, No.5, P.205-310.

Schultz P., S. Ronen, M. Hattori, and C. Corbett, "Seismic-Guided Estimation of Log Properties, Part 2", The Leading Edge, June 1994, Vol. 13, No.6, P. 674-678.

Schultz P., S. Ronen, M. Hattori, and C. Corbett, "Seismic-Guided Estimation of Log Properties, Part 3", The Leading Edge, June 1994, Vol. 13, No.7, P. 770-775.

Taner M.T. and R.E. Sheriff, "Application of Amplitude, Frequency, and Other Attributes to Stratigraphic and Hydrocarbon Determination", AAPG, Memoir 26, 1997, P.301-327.

Taner M.T., "Seismic Data Processing for Stratigraphic Objectives", Presented at the 23rd Annual OTC in Houston, Texas, May 6-9, 1991.

Taner M.T., "Seismic Attributes Revisited", Seismic Research Corporation, 1994.

Widess M.B. "How Thin is a Thin Bed?", Geophysics, Vol.38, No.6, Dec.1973, P.1176-1180.

Yoshioka K., N. Shimada, and Y. Ishii, "Application of Neural Networks and Cokriging for Predicting Reservoir Porosity-Thickness", GeoArabia, Vol.49, No.4, Apr.1984, P.344-352.

TEST TARGET (QA-3)

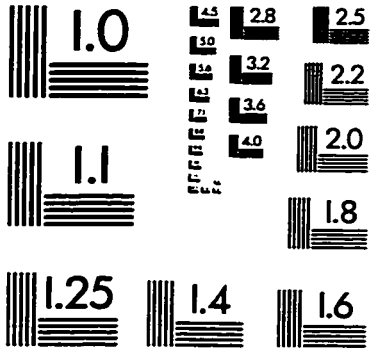

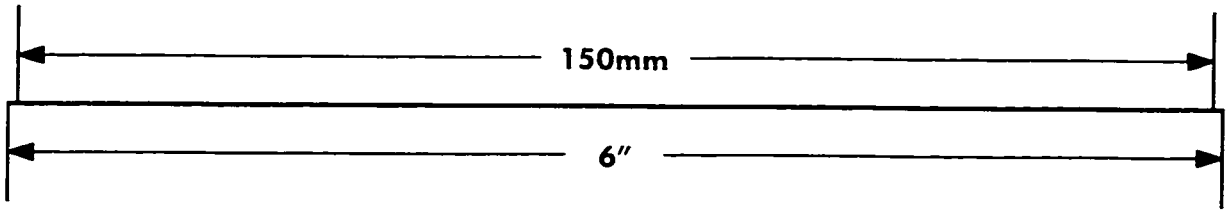

APPLIED IMAGE, Inc
1653 East Main Street
Rochester, NY 14609 USA
Phone: 716/482-0300
Fax: 716/288-5989